Universidade de Lisboa

Faculdade de Ciências

Departamento de Biologia Vegetal

Engineering new bacterial dye-decolourising peroxidases for lignin degradation

Diogo Alexandre Martins Aires Tavares

Dissertação

MESTRADO EM MICROBIOLOGIA APLICADA

2014

Universidade de Lisboa

Faculdade de Ciências

Departamento de Biologia Vegetal

Engineering new bacterial dye-decolourising peroxidases for lignin degradation

Diogo Alexandre Martins Aires Tavares

Dissertação

MESTRADO EM MICROBIOLOGIA APLICADA

Orientadores:

Professora Lígia Oliveira Martins, Instituto de Tecnologia Química e Biológica, UNL

Professor Rogério Tenreiro, Orientador Interno designado pela Faculdade de Ciências, UL

2014

Engineering new bacterial dye-decolourising peroxidases for lignin degradation

Diogo Alexandre Martins Aires Tavares

2014

The work presented in this thesis was conducted at the Instituto de Tecnologia Química e Biológica, in the Microbial and Enzymatic Technology (MET) Lab under the supervision of Professor Lígia Oliveira Martins and co-supervision of Dr. Vânia Brissos.

Table of contents

Acknowledgments ..... **iii**

Abstract ..... **iv**

Resumo ..... **v**

Abbreviations ..... **viii**

1. Introduction **1**

1.1 Peroxidases 2

1.2 Directed evolution 4

1.3 Directed evolution of PpDyP 6

2. Material and Methods **7**

2.1 Bacterial strains, plasmids and media 8

2.2 Preparation of electrocompetent cells 8

2.3 Selection of the appropriate enzyme substrate for activity screenings 8

2.4 Random mutagenesis by error-prone PCR (ep-PCR) 9

2.5 Recombination by DNA Shuffling and mutant library construction 10

2.6 Transformation of *E. coli* cells 11

2.7 Overexpression of *ppDyP* variants in 96-well plates 11

2.8 Cell disruption in 96-well plates 11

2.9 High-throughput screening for activity and stability 12

2.10 Production and purification of recombinant PpDyP variants 12

2.11 Spectroscopic analysis 13

2.12 Kinetic analysis 13

2.13 Enzyme kinetic stability 14

3. Results and Discussion **15**

3.1 Directed Evolution of PpDyP 16

3.1.1 Validation of high-throughput screenings 16

3.1.2 Selection of appropriate recombinant strains for enzymatic activity assays 16

3.1.3 Cell growth, cell disruption and activity assays in 96-well plates 17

3.1.4 Library construction by epPCR 18

3.1.5 Directed evolution of PpDyP 19

3.2 Spectroscopic and Biochemical Characterization of PpDyP Wild-type and Variants 27

3.2.1 Spectroscopic characterization 27

3.2.2 Kinetic properties 29
3.2.3 Kinetic Stability of PpDyP variants 31
3.3 Structural analysis of mutations 32
4. Conclusions 34
5. References 35

Acknowledgments

Quero agradecer a todas as pessoas que tornaram possível a elaboração desta dissertação de mestrado:

À minha orientadora, Professora Lígia Martins, por me ter aceite no seu laboratório, e me ter feito sentir como se estivesse em casa. Quero agradecer também as suas ‘’dicas’’ e, acima de tudo, a transmissão de conhecimento, e pela minha formação como investigador e pessoa.

À Dra. Vânia Brissos, por todo o acompanhamento ao longo do trabalho, pelas horas ‘’perdidas’’, pela determinação e encorajamento que teve sempre para comigo. E claro pelos ‘’puxões de orelhas’’ que me fizeram melhorar e aprender. O meu muito obrigado por toda a dedicação.

Ao Professor Rogério Tenreiro, por ter aceite ser o meu Orientador Interno, e pela disponibilidade demonstrada.

Aos membros do MET Lab: Sónia Mendes, que sempre me apoiou e ajudou no que podia, estando sempre disponível, obrigado também pela companhia no sempre relaxante chocolate a meio da tarde. Ao Joaquim Madeira (a.k.a. Jakas), pela amizade, companheirismo, encorajamento, passes para golo no futebol, e claro por me ouvir e compreender. À Lúcia Sabala (a.k.a Turbinada), pelas parvoíces e distracções quando eu ‘’estava em stress’’. A todos os outros que passaram pelo laboratório neste último ano, Marcelo, Bruna, Kamil, Marcin e Antonieta, o meu muito obrigado.

Aos meus colegas de mestrado, ‘’os fixes’’, Joana Carrilho, Margarida Duarte, Hélder Ribeiro, Diogo Dias, Bruno Arez e Inês Basto, o meu muito obrigado pela companhia, pelos jantares, pelas saídas, pelas distracções, e acima de tudo pela grande amizade. À Joana tenho de fazer um agradecimento extra, pela paciência e carinho incondicional.

Finalizar agradecendo à minha família, Mãe, Pai, Mano, Avó Fernanda, Tio Nuno, Tia Elsa e Prima Inês, fico-lhes agradecido por todo o apoio e coragem que me deram. Tenho a certeza que sem eles, não seria possível estar a escrever estes agradecimentos, porque simplesmente não teria uma tese onde os escrever.

Abstract

Dye-decolourising peroxidases (DyPs) are a novel family of heme-containing peroxidases showing a high efficiency for a wide number of substrates, including synthetic dyes, lignin units and metals, and are thus very attractive biocatalysts for application in the environmental and industrial biotechnology fields.

In this work high-throughput protocols were optimized and validated for the application of directed evolution approaches targeting PpDyP from *Pseudomonas putida* MET94 at the level of cell growth, lysis and enzymatic assays. Libraries of variants were created by epPCR and DNA shuffling techniques and explored for activity using high-throughput screenings activity assays. Four libraries of variants in a total of 8163 clones were explored in three rounds () of molecular evolution rounds to improve the efficiency for substrates and stability of PpDyP. The best variants were overproduced and purified and their structural and catalytic properties were characterized by spectroscopic and kinetic approaches. One variant, 21G11, was achieved showing 25- and 6-fold higher specificities (k_{cat}/K_m) for ABTS oxidation and H_2O_2 reduction, respectively. Importantly, variant 6E10, showing a 250-fold enhanced specificity for phenolics as compared with the wild-type was selected with a pH_{opt} = 5.4, 1.1 units up-shifted in relation to the wild-type enzyme.

Noteworthy a 2-fold increase in the protein production levels in relation to the wild-type was observed in both hit variants most probably related with the replacement of residue His125, for either a Arginine or Threonine, suggesting that this residue is a hot-spot in the enzyme structure to improve the protein production. Based in the model structure of PpDyP we have rationalized the structural molecular basis for increased activity for ABTS or DMP and improved kinetic stability and production yields of the PpDyP enzyme.

. .

Keywords: Dye-decolourising peroxidases, *Pseudomonas putida*, directed evolution, error-prone PCR, high-throughput screening, kinetic and stability analysis.

Resumo

As '' dye decolourising peroxidases'' (DyPs) são uma nova família de peroxidases hémicas que utilizam H_2O_2 e apresentam uma especificidade alargada para diferentes substratos, sendo de destacar o seu enorme potencial oxidativo para compostos aromáticos, tais como corantes sintéticos e unidades de lenhina fenólicas e não fenólicas.

Devido à especificidade alargada, as DyPs podem ser utilizadas como biocatalizadores em diferentes aplicações biotecnológicas. Todos os anos 800 mil toneladas de corantes sintéticos são produzidos e ~ 15% são libertados para os efluentes. Os tratamentos convencionais para a remoção destes corantes dos efluentes são atualmente pouco eficazes e muito dispendiosos. Devido à grande capacidade oxidativa das DyPs, estas enzimas têm um grande potencial para serem utilizadas no tratamento destes efluentes. Noutro contexto, a biorefinaria de lignocelulose poderá vir a ser uma solução para reduzir a utilização de matérias primas fósseis, não renováveis, com implicações no aquecimento global, para a produção de biocombustíveis, materiais e produtos de elevado valor acrescentado. Novamente, as DyPs ao mostarem capacidade oxidativa de unidades fenólicas e não-fenólicas de lenhina, poderão ter um papel importante, como enzimas ligninolíticas na degradação de material lignocelulósico muito resistente à degradação química e biológica.

As enzimas apresentam várias vantagens como catalizadores, são eficientes, específicas, seguras e amigas do ambiente, no entanto a sua eficiência e estabilidade por vezes ficam aquém das necessidades para a sua aplicação a nível industrial.

As proteínas podem ser melhoradas usando técnicas de engenharia racional no entanto esta abordagem requer um conhecimento extenso e muitas vezes inantingível da relação entre estrutura e função das proteínas. Para ultrapassar esta limitação surgiu uma tecnologia chave na área da engenharia molecular, denominada evolução dirigida, tendo mostrado resultados impressionantes no melhoramento de várias características dos biocatalisadores.

A evolução dirigida envolve 4 passos essenciais: (i) selecção do gene de interesse, (ii) construção da biblioteca de mutantes, (iii) selecção de proteínas mutantes com funções melhoradas, (iv) repetir o processo até o objectivo ser atingido. Os métodos mais comuns de mutagénese são a mutagénese aleatória, mutagenése por saturação e o "DNA shuffling''.

A mutagénese aleatória consiste em pequenas modificações dos protocolos de PCR, modificações essas, que aumentam a normal taxa de erro da enzima *Taq* polimerase. Normalmente estes protocolos contêm maiores concentrações de $MgCl_2$ em relação aos

tradicionais com o objectivo de estabilizar os pares não-complementares. A taxa de mutação também pode ser aumentada através da adição de $MnCl_2$ ou da variação do rácio de nucleótidos.

A mutagénese por saturação permite a criação de uma biblioteca de mutantes, que contém todas as mutações possíveis numa posição alvo da sequência da proteína. Desta forma um amino ácido pode ser substituído por todos os 20 amino ácidos introduzindo todos os codões possíveis nessa posição.

Por fim, o ‘’DNA shuffling” é uma técnica *in vitro* de recombinação aleatória dos mutantes seleccionados . O PCR reagrupa os genes a partir de fragmentos de DNA que são gerados por digestão aleatória prévia dos diferentes genes parentais.

Recentemente no Laboratório de Tecnologia Microbiana e Enzimática o gene que codifica para uma DyP de *Pseudomonas putida* MET94 (PpDyP) foi clonado, expresso, e a proteína foi super-produzida e purificada. Esta enzima mostrou ser eficiente na degradação de corantes azo e antraquinónicos e na oxidação de compostos fenólicos e não-fenólicos e iões metálicos como o manganês e o ferro. Esta especificidade alargada para diferentes substratos torna esta enzima muito atractiva para ser utilizada como biocatalizador nas áreas da biotecnologia ambiental e industrial.

O objectivo deste estudo foi estabelecer protocolos apropriados para a evolução dirigida da enzima PpDyP de form a então criar biocatalisadores de elevada performance para serem utilizados nas futuras biorefinarias. Nesse sentido, técnicas de evolução dirigida foram aplicadas à PpDyP. Quatro bibliotecas de mutantes, em três ciclos de evolução, foram construídas por técnicas de mutagénese aleatória e “DNA shuffling” e cerca de 8000 clones foram rastreados.

Os melhores mutantes de cada geração foram produzidos e purificados e as suas propriedades espetroscópicas e catalíticas foram estudadas. Espectroscópicamente todos os mutantes revelaram ser semelhantes à estirpe selvagem, o que indica que as mutações introduzidas não levaram a nenhuma alteração estrutural significativa da enzima. Durante o processo de evolução foram seleccionados variantes com especificidades distintas. Os mutantes 9F6 e 21G11 revelaram uma melhoria de 6 e 25 vezes na especificidade (k_{cat}/K_m) (1 ordem de grandeza) para os substratos ABTS e H_2O_2, respectivamente, quando comparados com a estirpe selvagem. A especificidade dos mutantes 17F11 e 6E10 aumentou cerca de 250 vezes (3 ordens de grandeza) para o substrato DMP quando comparados com a estirpe selvagem. Os mutantes 21G11 e 6E10 apresentaram um rendimento de produção proteica duas vezes superior relativamente à enzima nativa. Foi interessante verificar que ambos

adquiriram uma mutação na histidina125, sugerindo que este resíduo é um local importante para melhorar a produção da proteína.

Foi verificado também ao longo deste trabalho que é muito difícil aumentar simultaneamente a actividade catalítica e a estabilidade da enzima. Os mutantes 9F6 e 17F11 são bons exemplos, uma vez que o aumento da actividade catalítica resultou numa menor estabilidade. Isto deve-se provavelmente ao compromisso que existe entre a actividade e a estabilidade proteica. Inúmeras vezes para continuar a melhorar a actividade catalítica de um variante têmde ser introduzidas previamente mutações neutras importantes na estabilização da estrutura. Introduzindo posteriormente novas mutações que melhorem a actividade catalítica da enzima.

Neste trabalho a PpDyP foi evoluída com sucesso por técnicas de evolução dirigida, para maior capacidade oxidoreductiva para o ABTS, H_2O_2 ou para os compostos fenólicos e níveis de rendimento de produção melhorados.

Palavras-Chave: ‘’Dye-decolourising” peroxidases, *Pseudomonas putida,* evolução dirigida, mutagénese aleatória, ‘’high-throughput screening’’, análise cinética e de estabilidade

Abbreviations

ABTS – 2,2'-azino *bis* (3- ethylbenzthiazoline-6-sulfonic acid)

BSA – Bovine Serum Albumin

DMP – 2,6-Dimethoxyphenol

DyP – Dye decolourising peroxidase

epPCR – Error prone PCR

IPTG – isopropyl β-D-1-thiogalactopyranoside

LB – Luria-Bertani

MB9 - Mordant Black 9

OD_{600nm} – Optical density at 600 nm

RB5 – Reactive Blue 5

SDS-PAGE – Sodium dodecyl sulfate polyacrylamide gel electrophoresis

SOB – Super Optimal Broth

TB - Terrific Broth

UV – Ultra-violet

Vis – Visible

Wt – Wild-type

1. Introduction

1.1 Peroxidases

Heme peroxidases catalyze the H_2O_2-dependent oxidation of a variety of small organic substrates, playing multiple physiological roles in a wide range of living organisms. These enzymes were originally classified into two superfamilies: the plant peroxidases and the animal peroxidases (Welinder *et al.*, 1992). The fungal and bacterial peroxidase were lately included in the plant peroxidase superfamily and further classified into classes I, II, and III, based on primary structural homology. Class I is composed by intracellular prokaryotic peroxidases, including yeast cytochrome *c* peroxidase and chloroplast ascorbate peroxidase. Class II comprises extracellular fungal peroxidases, like lignin peroxidases, manganese peroxidases, and versatile peroxidases. Class III represents extracellular algae and plant peroxidases, such as horseradish peroxidases (Hofrichter *et al.*, 2010). Mammalian peroxidases have been recognized to constitute a separate peroxidase superfamily, the peroxidase-cyclooxygenase superfamily. They arose independently from the plant, fungal and (archae)bacterial superfamily as is inferred by substantial differences in sequence, overall structure and the nature of their prosthetic group, in which the ferri-protoporphyrin IX derivative is covalently linked to the protein (Zederbauer *et al.*, 2007). The main clades are represented by myeloperoxidases, eosinophil peroxidases and lactoperoxidase. They figure prominently in human biology and contribute to host defense against infection, hormone synthesis, and pathogenesis.

Recently a new family of peroxidases, known as the dye-decolourising peroxidases (DyPs) family, was proposed (Kim and Shoda, 1999). DyPs were first discovered in fungi, and later in a wide range of bacterial strains. DyP-type peroxidases are not considered members of plant or animal peroxidases because of their unique reaction characteristics and specific primary and tertiary structures (Sugano, 2009). These enzymes are sub-classified into the phylogenetically distinct classes A, B, C, and D (Colpa *et al.*, 2014). Class A contain a Tat-dependent signal sequence, which suggests that they function outside of cytoplasm or even extracellularly (Jongbloed *et al.*, 2004). Classes B and C are cytoplasmic enzymes, probably involved in intracellular metabolism. Class D contains primarily fungal enzymes. DyP-type peroxidases bind the heme cofactor non-covalently, as plant peroxidases.

All DyP peroxidases contain the so-called GXXDG motif in their primary sequence, which is part of the heme-binding region. The crystal structures of DyPs shows two domains with each domain consisting of a four-stranded antiparallel β-sheet and peripheral α-helices with the heme cofactor clefted in between (Figure 1A) distinct from the classic peroxidases that are primarily α-helical proteins (Zubieta *et al.*, 2007a; Zubieta *et al.*, 2007b; Liu *et al.*, 2011; Yoshida *et al.*, 2011; Singh *et al.*, 2012; Strittmatter *et al.*, 2013). A detail of the amino acid residues in the DyPs heme environment is shown in Figure 1B. DyPs lack the distal His, which is highly

conserved among classical peroxidases and is proposed to act as an acid/base catalyst in the catalytic mechanism. Instead, they house an Asp together with an Asn and an Arg. On the proximal side, the heme iron is coordinated by a His hydrogen bonded to an Asp residue, forming a Fe-His-Asp triad.

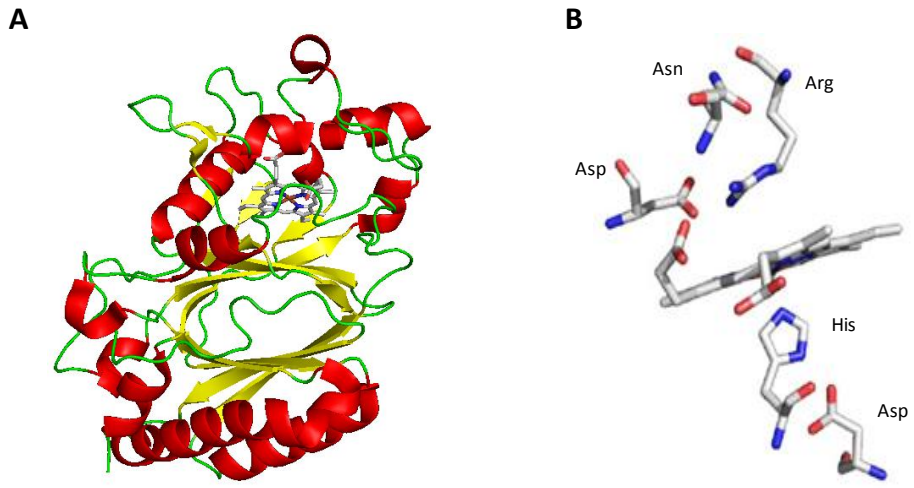

Figure 1 – (A) Crystal structure of TyrA (PDB 2iiz). The α helices are shown in red and the β sheets in yellow. **(B)** Representation of the catalytically distal and proximal residues important for the peroxidase activity. DyPs houses a distal aspartate (Asp), asparagine (Asn) and an arginine (Arg) and a proximal histidine (His) and an aspartate (Asp) (Santos *et al.*, 2014).

Considering their broad specificity, DyPs can be potentially used as biocatalysts in many different biotechnological applications (Colpa *et al.*, 2014). Every year 800,000 t of synthetic dyes are produced and ~ 15% are released into effluents. The removal of these dyes from effluents by conventional wastewater treatments is very expensive and technically challenge. Dye-containing effluents cause deterioration of water quality and become a health threat because of their mutagenic or carcinogenic properties (Rodriguez-Couto, 2009). DyPs shows potential for the set-up of enzymatic treatment of dye-containing wastewaters. Recently, the lignocelluloses biorefinery concept is receiving considerable attention as a source of a renewable chemicals, materials, and flues for future sustainable development. The lignocelluloses biorefinery should contribute to reduce the effects of global warming, caused by the consumption of crude oils, providing the production of biofuels (Martinez *et al.*, 2009). DyPs have the ability to act as ligninolytic enzymes, with potential to exert a crucial role in the oxidation of phenolic and non-phenolic lignin units since the lignocellulosic material is highly resistant to (bio)chemical degradation (Bugg *et al.*, 2011). Moreover, it was also shown that DyPs can be important in the degradation of β-carotene, with direct implications in food industry, enabling the enzymatic whitening of whey-containing foods and beverages (Scheibner *et al.*, 2008).

1.2 Directed evolution

Enzymes are biocatalysts, capable of carrying out a tremendous range of biochemical functions, however their efficiency, stability and costs often do not correspond to the needs of industry (Bloom *et al.*, 2005). One approach to engineering enzymes towards improved properties is to use rational design however, this approach requires an extensive and frequently unattainable knowledge of the relationship between structure and function of proteins (Kuchner and Arnold, 1997). An evolutionary engineering, named ''directed evolution'', has emerged as a key technology for biomolecular engineering, generating impressive results (Reetz *et al.*, 2008).

Direct evolution involves four keys steps: (i) select a starting gene sequence, (ii) create a library of variants, (iii) select variants by high-throughput screening with improved function, (iv) repeat the process until the improvement or function is achieved (Romero and Arnold, 2009). The most common mutagenesis method are error-prone PCR (epPCR), saturation mutagenesis and DNA shuffling (Tracewell and Arnold, 2009).

Error-prone PCR protocols consist in small modifications of the standard PCR methods in order to enhance the natural error rate of *Taq* polymerase. The epPCR protocols usually contain high concentrations of $MgCl_2$, in order to stabilize non-complementary pairs. Other ways to increase the mutation rate includes the variation of the nucleotides ratios or the addition of $MnCl_2$ to the reaction (Cirino *et al.*, 2003). Due to its simplicity and versatility, this epPCR has emerged as the most common technique and can result in mutation frequencies as high as 2% per nucleotide position (Brakmann, 2001).

Saturation mutagenesis enables the creation of a library of mutants containing all possible mutations at one or more pre-determined target positions in a gene sequence (Tracewell and Arnold, 2009). This is achieved by introducing all possible base triplets at a given codon, thereby resulting in the insertion of all 20 amino acids at this position of the protein. This method restricts the random mutations to predicted sites in the enzyme creating therefore what is called focused libraries, but requires structural information in order for the correct mutagenesis sites to be chosen (Reetz *et al.*, 2008). Since random point mutagenesis can not access a large fraction of the enzyme sequence, this technique is normally used to increase the number of amino acid substitutions accessible by random mutagenesis (Georgescu *et al.*, 2003).

DNA shuffling performs random *in vitro* recombination of gene variants created by random mutagenesis. It employs the PCR reassembly of whole genes from a pool of short overlapping DNA sequences that are generated by random enzymatic fragmentation of different parental genes (Brakmann, 2001).

The directed evolution method is highly versatile (Dougherty and Arnold, 2009), and has being successfully applied to improve several enzymatic properties, e.g. gene expression levels of a horseradish peroxidase (Lin *et al.*, 1999; Morawski *et al.*, 2000), protein stability of an azoreductase from *Pseudomonas putida* and a versatile peroxidase from *Pleurotus eryngii* (Garcia-Ruiz *et al.*, 2012; Brissos *et al.*, 2014) and enzymatic activity of a peroxygenase (Molina-Espeja *et al.*, 2014).

1.3 Directed evolution of PpDyP

Recently in Microbial and Enzymatic Technology (MET) Lab the gene coding for DyP from *Pseudomonas putida* MET94 (PpDyP) was cloned and expressed and the protein overproduced and purified showing a wide substrate specificity, including high redox potential aromatic compounds such as synthetic dyes, phenolic and nonphenolic lignin units and metal ions such as manganese and ferrous (Santos *et al.*, 2014). This enzyme has an optimal pH in the acidic range (pH 4-5) and showed higher activity between 10 and 30ºC. Considering the broad specificity, this enzyme has a considerable potential in the fields of environmental and industrial biotechnology.

However, peroxidases are not well-suited for industrial uses that generally requires particular substrate specificities and application conditions (pH and temperature) in addition to high expression levels (Martinez *et al.*, 2009). PpDyP is not an exception, and protein engineering techniques need to be applied to obtain highly gene expression levels, and to increase the protein stability and enzymatic activity.

Therefore, the major aim of this thesis was to create potential useful biocatalysts in the biorefinery field, evolving PpDyP towards higher activity for phenolic compounds by using directed evolution approaches. Libraries of variants were created by epPCR and DNA shuffling techniques and explored for activity using high-throughput screenings. The best variants were overproduced and purified and their structural and catalytic properties were addressed by spectroscopic and kinetic approaches.

2. Material and Methods

2.1 Bacterial strains, plasmids and media

Escherichia coli strain DH5α (Novagen) was used for routine propagation and amplification of plasmid constructs. *E. coli* Tuner (DE3, Novagen), KRX (Promega) and BL21 star (DE3, Novagen) strains were used to express the *ppDyP* wild-type (Wt) and variant genes cloned in pET21-21a (+) plasmid (Novagen). In the Tuner and BL21 star strains the target genes are under the control of T7 promoter, induced by isopropyl β-D-1-thiogalactopyranoside (IPTG) and in the KRX strain, the genes are under the control of rhaP_{BAD} promoter, induced by rhamnose. Luria-Bertani medium (LB) and Terrific Broth medium (TB) were used for the maintenance and growth of *E. coli* strains, supplemented with 100 µg/mL ampicillin. LB medium contains (per liter): 10 g of tryptone, 5 g of yeast extract and 10 g of $NaCl_2$. TB medium contains the following components (per liter): 12 g of tryptone, 24 g of yeast extract, 3.4 g of glycerol, 2.3 g of KH_2PO_4 and 12.5 g of K_2HPO_4. Super Optimal Growth medium (SOB) was used for the growth of competent cells. SOB medium contains (per liter): 20 g of tryptone, 5 g of yeast extract, 0.584 g of $NaCl_2$ and 0.186 g of KCl_2. All culture media were sterilized in an autoclave and stored at room temperature.

2.2 Preparation of electrocompetent cells

A LB agar plate was streaked out with *E. coli* KRX cells and incubated overnight at 37ºC. A single colony was picked, used to inoculate 20 mL of SOB medium and incubated overnight at 37ºC at 120 rpm. Growth at a scale of 500 mL in SOB medium was started with an optical density at 600 nm (OD_{600nm}) of 0.05 and incubated at 37ºC, with 120 rpm. After 3.5 h (OD_{600nm} ~ 0.8), cells were transferred to ice-cold centrifuge bottles and spin down at 5,000 rpm for 15 min at 4ºC. The supernatant was discarded, and the cell pellet was washed with 500 mL of a sterile ice-cold 10% glycerol solution. The cells were centrifuged, re-washed in 500 mL of the same solution, centrifuged for a second time and re-suspended in the remained solution (~ 2.5 mL). Aliquots of 100 µL were frozen on nitrogen and stored at - 80ºC.

2.3 Selection of the appropriate enzyme substrate for activity screenings

Growth of recombinant strains and *ppDyP* overexpression

The plasmid pRC-1, containing the *ppDyP* gene, was transformed into *E. coli* Tuner (DE3, Novagen), KRX (Promega) and BL21 star (DE3, Novagen) strains (Santos *et al.*, 2014). Single colonies were used to inoculate 10 mL of LB medium supplemented with 100 µg/mL ampicillin, grown overnight at 37ºC, 160 rpm. Fresh cultures were transferred to 100 mL of LB medium supplemented with 100 µg/mL ampicillin, in order to start the growth with an OD_{600nm} = 0.05. Cultures were incubated at 37ºC, 160 rpm and when OD_{600nm} ~ 0.6, 100 µM IPTG was added to recombinant *E. coli* Tuner and BL21 star strains, and 0.1 % rhamnose to recombinant *E. coli*

KRX. After 24 h of cultivation, cells were collected by centrifugation (8,000 rpm, 10 min at 4ºC). The cell pellets were resuspended in 1 mL of 20 mM Tris-HCl buffer (pH 7.6), containing 5 mM $MgCl_2$, 1 U/mL of DNase I, and 2 µL/mL of a mixture of protease inhibitors, antipain and leupeptin. After cells were disrupted by French Press (Thermo EFC) and then centrifuged at 15,000 for 2 h at 4ºC. The supernatants (cell crude extracts) were collected and used for enzymatic assays. The protein concentration was determined using the Bradford assay with bovine serum albumin (BSA) as standard. SDS-PAGE electrophoresis was used to visualize protein overproduction in crude extracts.

Enzymatic assays

Enzymatic activities of PpDyP were monitored using a Nicolet Evolution 300 spectrophometer (Thermo Industries). The activities were measured by monitoring the oxidation of different substrates at their maximum absorption wavelengths in the presence of 0.2 mM H_2O_2 Enzymatic assays were performed at 30ºC, in 20 mM acetate buffer at pH 4.3 using 1 mM of 2,2'-azino *bis* (3-ethylbenzthiazoline-6-sulfonic acid) (ABTS), 1 mM guaiacol (ε_{470nm}=26,600 M^{-1} cm^{-1}) or 1 mM 2,6-Dimethoxyphenol (DMP) (ε_{468nm}=49,600 M^{-1} cm^{-1}), and at pH 5 using 0.1 mM of reactive blue 5 (RB5) (ε_{610nm}=7,690 M^{-1} cm^{-1}) or 0.1 mM mordant black 9 (MB9) (ε_{550nm}=15,641 M^{-1} cm^{-1}).

2.4 Random mutagenesis by error-prone PCR (ep-PCR)

Mutations in the *ppDyP* gene were generated by using error-prone PCR (ep-PCR). Primers 5'-GGATTAGCCT**CA'T**<u>**ATG**</u>CCGTTCCAGCAAGG-3' (PpDyP Forward) and 5'-GTGTTTCTGTATCT**G'GATCC**TTAGAGATCAGGCCCGC-3' (PpDyP Reverse) flanking the gene beyond the *Nde*I and *Bam*HI sites were used for amplification. ep-PCR was carried out in 50 µL reaction volume containing 3 ng of DNA template, 0.5 µM of primers, 200 µM of dNTPs, 7 mM $MgCl_2$, *Taq* polymerase buffer and 5 U of *Taq* polymerase (Fermentas). The effect of $MnCl_2$ concentration (0.01-0.25 mM) in the mutation rate was assessed. After an initial denaturation period of 10 min at 94ºC, the following steps were repeated for 28 cycles in a thermal cycler (MyCycler™ thermocycler, Biorad): 1 min at 94ºC, 1 min at 57ºC and 1.5 min at 72ºC and at the end 10 min at 72ºC. The amplified product (5 µL) was visualized by agarose (1%) electrophoresis, purified using the GFX PCR DNA and the Gel Band Purification kit (GE Healthcare) and eluted with mili-Q H_20. Ten microliters of purified PCR product and 10 µL of plasmid pET-21a (+) (Novagen) were digested with 10 U of *Nde*I (Fermentas) at 37ºC for 2 h. The mixture was placed at 65ºC for 20 min and then dialyzed against milli-Q H_20 for 30 min using MF™ filters (Milipore). A second digestion was performed with 10 U of *Bam*HI (Fermentas) for 2 h at 37ºC, and pET-21a (+) was simultaneously dephosphorylated with 1 U Alkaline Phosphatase (FastAP, Fermentas), to prevent plasmid self-ligation. The products

were purified using GFX PCR DNA and the Gel Band Purification kit (GE Healthcare). The ligations were performed with 0.5 U of T4 DNA ligase (Fermentas) using a ratio of 1:8 of vector to insert. This mixture was incubated overnight, at room temperature then incubated at 65ºC for 20 min. The preparation was then dialyzed against mili-Q H_20 for 30 min using MF™ filters (Milipore). After that 5 µL of this mixture was used to transform electrocompetent *E. coli* KRX cells.

2.5 Recombination by DNA Shuffling and mutant library construction

DNA shuffling was performed using PpDyP variants, 21G11, 5B9, 22B3, 9G8, 27B3. The mutant ppDyP genes were amplified by PCR using primers pET21F (5'-CTTCCCCATCGGTGATGTCGGCGATATAG-3') and pET21R (5´-CCAAGGGGTTATGCTAGTTATTGCTCAG-3'). A mixture containing 200 ng of each parental gene was digested with 0.05 U/ µL of DNase I in a 200 mM Tris-HCl buffer, pH 7 with 80 mM $MnCl_2$ for 7 min at 15ºC in a thermocycler (MyCycler™ thermocycler, Biorad). Digestion was stopped by adding 6 µL of 50 mM EDTA. The PCR reassembly was carried out in a 20 µL reaction volume containing 3 µL of DNA fragments, 200 µM of dNTPs, NZYProof polymerase buffer and 2.5 U of NZYProof Polymerase (NZYTech). After an initial denaturation period of 3 min at 96ºC, the following steps were repeated for 45 cycles in a thermal cyler (MyCycler™ thermocycler, Biorad): 1 min at 94ºC, 90 s at 59ºC, 90 s at 56ºC, 90 s at 53ºC, 90 s at 50ºC, 90 s at 47ºC, 90 s at 44ºC, 90 s at 41ºC, and 1 min + 5 s/ cycle at 72ºC followed by a final 10 min period at 72ºC. The PCR reassembly products were amplified by PCR using primers 5'-GGATTAGCCT**CA'T**<u>**ATG**</u>CCGTTCCAGCAAGG-3' (PpDyP Forward) and 5'-GTGTTTCTGTATCT**G'GATCC**TTAGAGATCAGGCCCGC-3' (PpDyP Reverse). PCR was carried out in a 50 µL reaction volume containing 1 µL of PCR reassembly products, 1 µM of primers, 200 µM of dNTPs, 0.01 mM of $MnCl_2$, NZYProof polymerase buffer and 2.5 U of NZYProof Polymerase (NZYTech). After an initial denaturation period of 3 min at 94ºC, the following steps were repeated for 20 cycles in a thermal cyler (MyCycler™ thermocycler, Biorad): 30 s at 94ºC, 1 min at 55ºC, 90 s at 72ºC followed by a final 10 min period at 72ºC. The amplified products were purified using GFX PCR DNA and the Gel Band Purification Kits (GE Healthcare). The final PCR products were digested with *Nde*I/*Bam*HI (Fermentas), and cloned into pET-21a (+) (Novagen) as described above. Ligation reaction mixtures were used to transform electrocompetent *E. coli* KRX cells.

2.6 Transformation of *E. coli* cells

One or five microliters of purified plasmids or ligation mixtures, respectively, were added to an aliquot of 100 µL electrocompetent cells (previously thawed on ice) mixed and placed on ice for 5 min. This mixture was transferred to a sterile and ice-cold electroporation cuvette, which was placed in the Xcell ShockPod chamber (Gene Pulser Xcell™, Biorad) and pulsed using set conditions C = 25 µF, PC = 200 Ω, V = 2.5 kV. One mL of LB medium was immediately added and the suspension was transferred to an Eppendorf, and incubated at 37ºC for 1 h at 200 rpm. The cells were then centrifuged at 5,000 rpm for 5 min; 0.9 mL of supernatant was discarded and the cells were re-suspended in the remaining medium (~ 0.1 mL). The cells were spread on a LB agar plate, supplemented with 100 µg/mL of ampicillin and incubated overnight at 37ºC.

2.7 Overexpression of *ppDyP* variants in 96-well plates

From a fresh agar plate, individual colonies were randomly picked and transferred to a 96-well plate (Greiner Bio-One) containing 200 µL of LB medium supplemented with 100 µg/mL ampicillin. In order to avoid evaporation only the interior wells were used while peripheral wells were filled with sterilized water and the plates were sealed with a foil. Four wells in each plate were used to inoculate the parent of each generation (in which WT was the parent of the 1st generation). Cultures were grown for 24 h at 30ºC, 750 rpm in a Titramax 1000 shaker (Heidolph). Twenty microliters aliquots were used to inoculate 180 µL of TB medium supplemented with 100 µg/mL ampicillin. The 96-well plate were sealed with parafilm and incubated at 30ºC, 750 rpm. After 4 h of incubation, 0.2% rhamnose and 15 µM hemin were added to induce gene expression, and the growth proceeded for a 24 h period. The cells were harvested by centrifugation at 4,000 rpm, for 30 min at 4ºC.

2.8 Cell disruption in 96-well plates

Three different methods were tested for cell disruption. First in the **chemical** cell disruption method, 100 µL of a 40% Bacterial Protein Extraction Reagent (B-PER®) lysis solution (Thermo Scientific) was used to re-suspend the cell pellets. In the **physical** method, 96-well plates were submerged in liquid nitrogen and then thawed at room temperature for 5 min. After 3 cycles of freeze and thaw, cell pellets were re-suspended in 100 µL of 20 mM Tris-HCl, pH 7.6. The third method combined both a **physical** and **enzymatic** approach; 96-well plates were frozen at - 80ºC for 15 min and then thawed at 30ºC for 5 min. After 3 cycles of freeze and thaw, cell pellets were re-suspended in 100 µL of 20 mM Tris-HCl, pH 7.6, and lyzozyme (2 mg/mL) was added. After cell disruption, plates were centrifuged at 4,000 rpm, for 30 min, at 4ºC and the supernatant collected (crude extracts) and used for enzymatic activity measurements.

2.9 High-throughput screening for activity and stability

Cell crude extracts (20 µL) were transferred to a new 96-well plate using a Liquid Handling High-Throughput robot (Hamilton), and initial activity (A_i) was measured by adding 180 µL of 20 mM acetate buffer at pH 4.3 containing 0.2 mM H_2O_2 and 1 mM ABTS or 1 mM DMP. The oxidation was followed on a Synergy 2 (BioTek) micro plate reader. After 2.5 h a new reaction was performed using the crude extracts in order to test the residual activity of variants ($A_{2.5h}$). Between the two measurements the crude extracts were stored at 4ºC.

The activity of each variant in relation to the parent enzyme was calculated using the ratio of the initial activity of the variant (v) to the parent (p) (A_{i_v}/Ai_p). The stability values were calculated using the ratio of the residual activity after 2.5 h to the initial activity of the variant, normalized to the parent type $(A_{2.5h}/A_i)_v/(A_{2.5h}/A_i)_p$. The variants exhibiting the highest activity or stability were selected and re-screened, to rule out false positives. The selected hit variants from each generation were grown overnight in 10 mL LB medium supplement with 100 µg/mL of ampicillin, at 37ºC, 120 rpm. The plasmidic DNA was extracted by using GeneJET Plasmid Miniprep Kit (Thermo Scientific) and mutations identified by DNA sequencing analysis. To identify the codons exchanges and amino acids substitutions, the Basic Local Alignment Search Tool (BLAST) was used. In each generation, the parent for the next generation was chosen among the variants showing the highest initial activity and/or stability.

2.10 Production and purification of recombinant PpDyP variants

The production of PpDyP variants at a larger scale was performed as described above. Briefly, single colonies were used to inoculate 100 mL of LB medium supplemented with 100 µg/mL ampicillin, grown overnight at 37ºC, 150 rpm. Fresh cultures were transferred to 1 L of LB medium in 5 L-Erlenmeyer flasks, supplemented with 100 µg/mL ampicillin, in order to start the growth with an OD_{600nm} = 0.05. Cultures were incubated at 37ºC at 150 rpm and when OD_{600nm} ~ 0.6, 100 µM IPTG and 15 µM hemin were added to the growth. After 24h of cultivation, cells were collected by centrifugation (8,000 rpm, 15 min at 4ºC) and were disrupted in a French press. Cell debris was removed by centrifugation 15,000 rpm (3h, 4ºC) and crude extracts were used for protein purification in an AKTA purifier (GE Healthcare, BioSciences, Uppsala, Sweden) at room temperature (Santos *et al.*, 2014). The crude extract was loaded onto a Q-Sepharose column equilibrated with 20 mM Tris-HCl buffer, pH 7.6. Elution was carried out with 1 M NaCl in buffer. The active fractions were pooled and concentrated before applying on a Superdex 200 HR 16/60 column (GE Healthcare, BioSciences) equilibrated with 20 mM Tris-HCl buffer, pH 7.6 with 0.2 M NaCl. The purified protein was stored at -20ºC until it was used.

2.11 Spectroscopic analysis

The UV-visible absorption spectra of purified enzymes were recorded on a Nicolet Evolution 300 spectrophotometer from Thermo Industries (Madison, USA) at room temperature. The heme content was determined by the pyridine ferrohemochrome method using an extinction coefficient of $\varepsilon_{R\text{-}O\ 556nm}$ (28.32 mM^{-1} cm^{-1}) (Berry and Trumpower, 1987). In short, this method consisted in adding a solution of 500 µl pure protein, a stock solution of 0.5 mL solution containing 200 mM NaOH, 40% pyridine and 3 µl 0.1 M $K_3Fe(CN)_6$. This mixture was stirred and a spectrum was traced, corresponding to the oxidized protein. Thereafter sodium dithionite was added, the mixture stirred and a spectrum was traced again, corresponding to the reduced protein. The heme content was determined by the difference between the absorbance values at 556 nm of the oxidized and reduced protein spectra using the molar extinction coefficient of oxidized $\varepsilon_{R\text{-}O\ 556nm}$ at 28.32 mM^{-1} cm^{-1}.

2.12 Kinetic analysis

The enzymatic activity of PpDyP wild-type and variants was monitored using a Synergy2 microplate reader (BioTek, Vermont, USA). All enzymatic assays were performed at least in triplicate. The activity dependence on pH was measured by monitoring the oxidation of different substrates (ABTS, DMP, guaiacol, $FeSO_4$ and $MnCl_2$) at their maximal absorption wavelengths in the presence of 0.2 mM H_2O_2 at 25ºC using Britton-Robinson buffer (100 mM phosphoric acid, 100 mM boric acid, and 100 mM acetic acid mixed with NaOH to the desired pH in the range 2-11).

Apparent steady-state kinetic constants (k_{cat} and K_m) were measured. Reactions with $MnCl_2$ (0.1-3 mM) were performed in 50 mM sodium lactate at pH 5. The Mn^{3+} lactate formation was monitored at 270 nm ($\varepsilon_{270\ nm}$= 3,500 M^{-1} cm^{-1})(Kuan *et al.*, 1993). Fe^{3+} formation was monitored at 300 nm ($\varepsilon_{300\ nm}$= 2,200 M^{-1} cm^{-1}) upon reaction with $FeSO_4$ (0.05-1.5 mM), at optimal pH (pH 5 for PpDyP Wt, 9F6 and 21G11, and pH 6 for 17F11 and 6E10). The kinetic constants for H_2O_2 (0.005-5 mM) were measured in the presence of the 1 mM ABTS, at optimal pH (pH 4.3 for Wt, 9F6 and 21G11 and pH 5.4 for 17F11 and 6E10). The apparent steady-state kinetic constants for ABTS (0.1-5 mM) were performed at the optimum pH for each variant (pH 4.3 for Wt, 9F6 and 21G11 and pH 5.4 for 17F11 and 6E10) and also for the phenolic substrates guaiacol (0.001-3 mM) and DMP (0.001-1 mM), at their optimal pH (pH 4.3 for Wt, 9F6 and 21G11, and pH 8.4 for 17F11 and 6E10). Kinetic data were fitted directly into the Michaelis-Menten equation (Origin-Lab software, Northampton, MA, USA).

2.13 Enzyme kinetic stability

The enzymes were incubated at 40ºC in 20 mM Tris-HCl buffer, pH 7.6, and at fixed time intervals, samples were withdraw and tested for activity following the ABTS oxidation at 25°C. The assays were performed on a Nicolet Evolution 300 spectrophotometer from Thermo Industries (Madison, USA).

3. Results and Discussion

3.1 Directed Evolution of PpDyP

3.1.1 Validation of high-throughput screenings

The potential involvement of DyPs in the degradation or conversion of phenolics and recalcitrant methoxylated aromatics in lignin renders these enzymes very attractive for lignocellulosics related-applications. PpDyP is able to oxidise not only phenolic but also non-phenolic lignin units, (Santos *et al.*, 2014). The main goal of this work is to improve the PpDyP activity for phenolics compounds. These compounds can also be used as redox mediators for the oxidation of non-phenolic lignin units. In directed evolution experiments, a high number of information is generated in each generation. The precision of the high-throughput methods used is of an utmost importance in assessing the evolvability characteristics of the parental enzyme of each generation and the mutant libraries quality. These have a direct impact in the achievement of improved hits for the characteristic of choice (Salazar and Sun, 2003). The implementation of efficient screening protocols, in which a reduced risk of selecting false positives is achieved, is therefore essential and requires an optimization of each of several steps throughout the process. The variability among assays must be minimized during: (i) cell growth, (ii) cell lysis, and (iii) enzyme activity assays.

3.1.2 Selection of appropriate recombinant strains for enzymatic activity assays

The enzymatic activity in crude extracts of three recombinant *E. coli* strains overexpressing *ppDyP*, BL21 star, KRX and Tuner, was tested using as substrates, ABTS, the phenolic compounds, guaiacol and DMP, the azo dye, mordant black 9 (MB9), and the anthraquinonic dye, reactive blue 5 (RB5) (Table 1).

Table 1 – Specific activity of PpDyP towards different substrates using crude extracts of BL21 star, Tuner and KRX expressing the *ppDyP* gene. Enzymatic assays were performed at 30ºC, in 20 mM acetate buffer at pH 4.3 for ABTS, guaiacol and DMP (1 mM) and pH 5 for RB5 and MB9 (0.1 mM) in the presence of 0.2 mM H_2O_2.

		Specific Activity (nmol/min.mg)				
		ABTS	Guaiacol	DMP	RB5	MB9
BL21 star	Induced	160 ± 30	14 ± 3	*ND*	0.33 ± 0.17	3.8 ± 0.5
	Non-Induced	102 ± 7	9 ± 1.6	*ND*	0.05 ± 0.02	0.38 ± 0.06
Tuner	Induced	1421 ± 118	3 ± 1.8	20 ± 3	2 ± 0.52	12 ± 4
	Non-Induced	64 ± 6	1.2 ± 1.7	4.5 ± 1.6	0.28 ± 0.09	2.6 ± 4.5
KRX	Induced	3673 ± 837	*ND*	36 ± 7	*ND*	48 ± 15
	Non-Induced	778 ± 768	*ND*	20 ± 8	*ND*	25 ± 5

ND not determined

The results show that the enzymatic activities in crude extracts of recombinant strain BL21 star are in general lower than those measured using other *E. coli* strains. Moreover, no major differences are detected in the oxidation rates for ABTS and guaiacol in cells induced and non-induced (Table 1). The activities in crude extracts of induced recombinant strain Tuner are 3 to 22 times higher when compared to non-induced conditions for all the tested substrates. The recombinant strain KRX shows the highest activity for all the tested substrates and a reasonable variation between induced vs. non-induced conditions. Therefore KRX was selected for further studies. Moreover, KRX is a cloning as well as an expressing strain, which allows avoiding additional steps of plasmid transference during the laboratory evolution process.

3.1.3 Cell growth, cell disruption and activity assays in 96-well plates

E. coli KRX overexpressing the *ppDyP* gene was cultivated in LB and TB media in 96-well plates. The final OD_{600nm} was 1.0 ± 0.25 and 1.2 ± 0.1 for cell cultivation in LB and TB, respectively. The coefficient of variation (CV = standard deviation/ mean x 100%) was significantly lower in TB medium, ~ 8%, than in LB medium, ~ 30%. Cells grown in TB medium were therefore harvested by centrifugation and cell disruption procedures applied.

The B-PER® lysis solution, an easy and fast chemical lysis method, containing a mild and non ionic detergent, was first used. The protein concentration and enzymatic activities for ABTS as substrate were determined in crude extracts after cell lysis and very high coefficients of variation, 40 and 333%, for the protein content and enzyme activity, respectively, were measured ruling out the utilization of this method for cell disruption in subsequent experiments (Table 2).

Table 2 - Protein content and specific activity in crude extracts. Cells were disrupted using chemical (B-PER® lysis solution), physical (freeze/thaw using Liquid Nitrogen (LN)) or Physical + enzymatic (Lysozyme and Liquid Nitrogen or incubation at -80ºC) methods.

Disruption Method		Protein		Specific Activity	
		(mg/mL)	CV (%)	(nmol/min.mg)	CV (%)
Chemical	B-PER	0.5 ± 0.2	40	18 ± 60	333
Physical	Freeze/Thaw (LN)	0.3 ± 0.2	67	110 ± 266	266
Physical + Enzymatic	Freeze/Thaw (LN) + Lysozyme	0.4 ± 0.2	50	55 ± 115	209
	Freeze/Thaw (-80˚C) + Lysozyme	0.6 ± 0.1	17	117 ± 24	21

A physical method was then tested, in which the cell pellets were subjected to cycles of freezing and thawing. The 96-well plates were submerged in liquid nitrogen and thawed at room temperature, and the process was repeated 3 times. Using this disruption method the protein concentration in crude extracts was ~ 2-fold lower than those observed when chemical lysis was used (Table 2). Eventually the lower protein yields are due to limitations of the membrane pores size that are induced by freeze and thaw, that could likely retain proteins with large molecular masses (Johnson and Hecht, 1994). Additionally, the application of this method also resulted in high and unacceptable coefficients of variation, 67% for protein concentration and 266% for enzyme activity (Table 2). Interestingly by applying this methodology the specific activity is ~ 6 times higher when compared to the chemical method which could indicate that the detergent used in the latter method could result in PpDyP inactivation (Table 2).

In an attempt to improve this latter protocol cell pellets were re-suspended in a solution containing lysozyme (2 mg/mL), that hydrolyses the 1,4-β linkages connecting N-acetylmuramic acid and N-acetylglucosamine in peptidoglycan of bacterial cell walls, however the results achieved were similar (Table 2). Finally, instead of using liquid nitrogen we incubated the 96 well-plates at - 80°C for 15 min followed by thaw at 30°C for 5 min and the process was repeated 3 times. The cell pellets were then re-suspended with a solution containing lysozyme (2 mg/mL) for 5 min. This sequence resulted in highest protein concentrations and specific activities in cell extracts with the lowest coefficients of variation, 17 and 21%, respectively, as compared with the other methods and therefore was selected for further studies (Table 2).

3.1.4 Library construction by epPCR

Libraries of mutants were constructed by epPCR using *Taq* DNA polymerase and $MnCl_2$ concentration from 0.01 to 0.2 mM (Cirino *et al.*, 2003) to attain 1-3 amino acid changes (1-5 nucleotide substitution/gene) which corresponds roughly to 30 to 45% of the total number of clones with less than 10% of activity of the Wt (Salazar and Sun, 2003). .

Enzymatic assays were performed in three libraries constructed in the presence of 0.1 mM, 0.15 mM and 0.2 mM $MnCl_2$, however the number of inactive clones was ~ 80% in all of them. Therefore the concentration of $MnCl_2$ was decreased ~ 10 times and two other libraries with 0.01 mM and 0.02 mM $MnCl_2$ (Figure 2) were constructed. The percentages of clones with less than 10% of Wt activity was 30% and 52%, for the libraries with 0.01 mM and 0.02 mM $MnCl_2$, respectively (Figure 2). Therefore, 0.01 mM $MnCl_2$ was selected to create the PpDyP variant libraries.

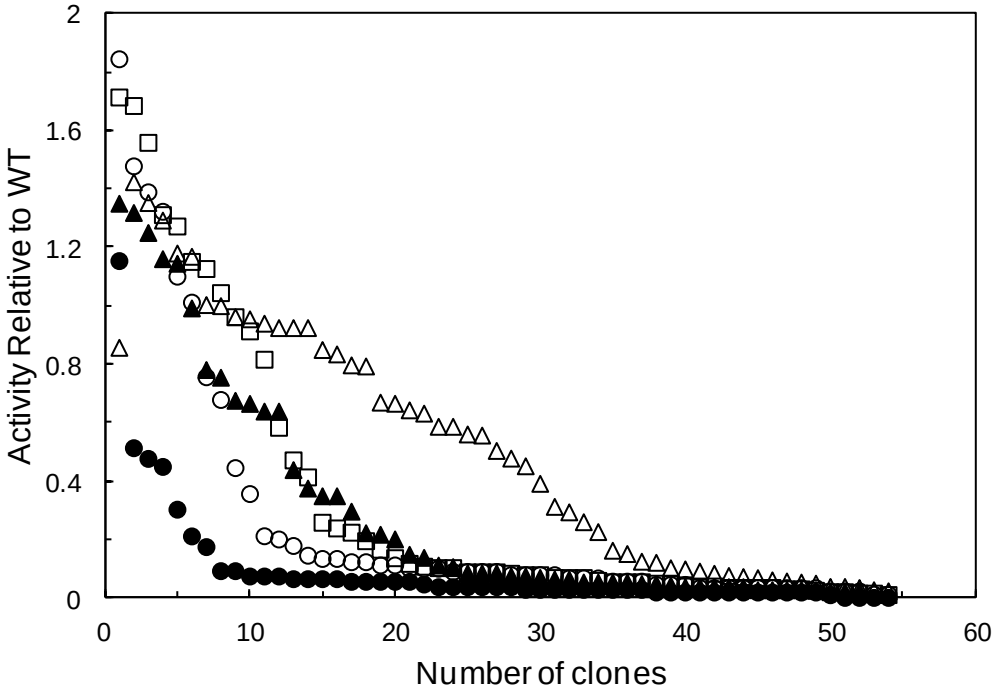

Figure 2 - Landscape for five variant libraries using different $MnCl_2$ concentration: 0.01 mM (△), 0.02 mM (□), 0.1 mM (▲), 0.15 mM (○), and 0.2 mM (●). Activity of clones relative to the Wt is plotted in descending order.

3.1.5 Directed evolution of PpDyP

3.1.5.1 Towards improved catalytic efficiency for phenolics

The specific activity for DMP in purified wild-type PpDyP is 100 times lower than that for ABTS (Table 1) (Santos *et al.*, 2014). Using crude extracts in 96-well plates no activity for DMP could be detected in wild-type and for this reason the first libraries were screened using ABTS as substrate. Additionally, it was observed a loss of enzymatic activity after leaving the crude extracts at 4°C for 2.5 h which might hinder the high-throughput screening protocols. Therefore a simultaneous screening for activity and stability was set-up using an incubation time of 2.5 h which resulted in a residual activity of about one-third of the initial activity (Garcia-Ruiz *et al.*, 2010).

In the 1st generation, a total of 1874 clones were screened (Figure 3A) and 16 variants were identified with improvements in initial activity and/or in stability and re-screened to rule out false positives (Figure 3B).

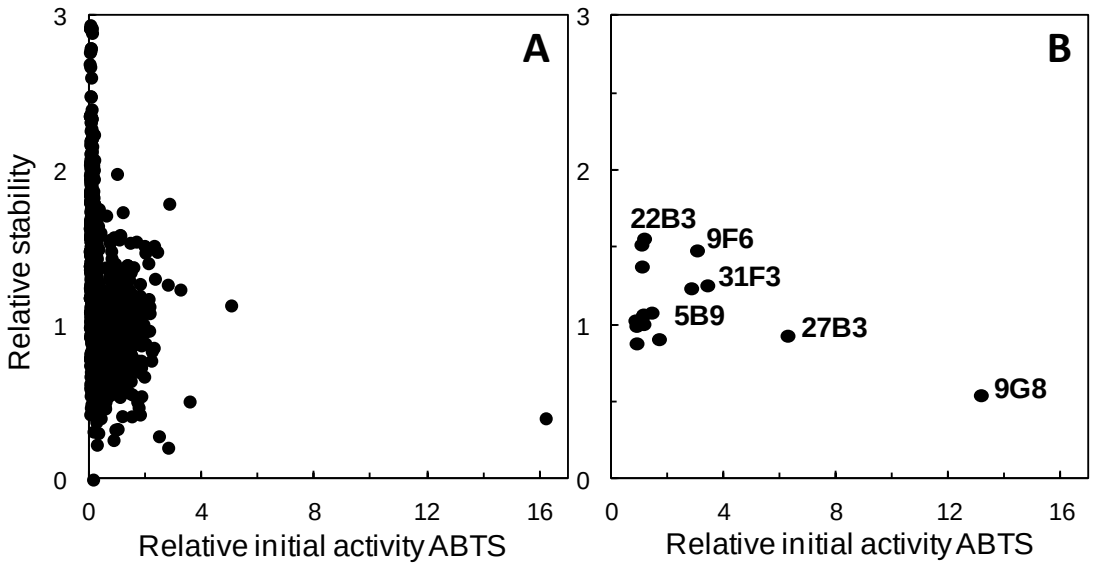

Figure 3 – Directed evolution landscape for the first generation mutant library. **A –** Initial activity vs stability of 1874 clones screened relative to the wild type. **B –** Re-screening of the best variants identified in the first generation. Stability is measured by the ratio of residual activity following incubation at 4°C for 2.5 h to initial activity.

Six variants were selected as hits: two variants, named 5B9 and 31F3, exhibited an improvement in the initial activity of around 3-fold when compared to the wild-type, while maintaining a similar stability (Table 3, Figure 3B). Another two variants, named 9G8 and 27B3, showed an improvement in initial activity of around 13-fold, and 6-fold, respectively, when compared to the wild-type however the stability, especially of the variant 9G8, was lower. The 22B3 variant exhibited a similar initial activity as compared with the wild-type, while the stability was improved about 1.6 times. The 9F6 variant showed an improvement in the initial activity and stability of around 3.5-fold and 1.5-fold, respectively, when compared to the wild-type. The best hits were also re-screened using DMP as substrate and only a residual activity could be detected in variant 9F6.

The DNA sequence information of the variants showed that the mutation rate was one substitution per gene, except in 9G8 variant, where two substitutions were found. The variants 5B9, 9F6, 22B3 27B3 and 31F3 revealed the following mutations, Q165R, E188K, S78G, H121Y and H125R, respectively, while variant 9G8 showed , H121Y and E209G mutations (Table 3).

The 9F6 variant was selected as parent for the 2nd generation of directed evolution, considering its best compromise between the activity and stability properties (Figure 4 and Table 3).

Table 3 – Summary of libraries amino acids substitutions accumulated in PpDyP variants and initial activity relative to their parents, using ABTS and DMP as substrates. Parents for the next generation are in bold for libraries constructed by epPCR and in italic for libraries constructed by DNA shuffling.

Generation	Variants	Mutations	Initial activity relative to parent[1)]		Stability relative to parent[2)]
			ABTS	DMP	(4°C, 2.5 h)
1st	**9F6**	E188K	3.7 ± 0.1	*r*	1.5 ± 0.2
	5B9	Q165R	2.8 ± 0.1	*nd*	1.2 ± 0.2
	9G8	E209G, H121Y	13.2 ± 0.3	*nd*	0.6 ± 0.1
	22B3	S78G	1.1 ± 0.2	*nd*	1.6 ± 0.1
	27B3	H121Y	6.3 ± 0.2	*nd*	1.0 ± 0.1
	31F3	H125R	3.4 ± 0.2	*nd*	1.2 ± 0.2
2nd	**17F11**	E188K, A142V	2.0 ± 0.05	3.0 ± 0.5	1.0 ± 0.05
	21G11	E188K, H125R	6.3 ± 0.3	1.5 ± 0.6	1.0 ± 0.1
3rd	6E10	E188K, A142V, H125T	2.0 ± 0.1	3.5 ± 0.2	[3)]
3rd	2F3	V12L, L23P, R65S, E188K, I254V	3.1 ± 0.4	1.2 ± 0.2	*ND*
(DNA shuffling)[4)]	3E10	H121Y, V241E	4.5 ± 0.5	*nd*	*ND*
	5E11	H121Y, E188K, E209G, W270R	3.5 ± 0.4	1.4 ± 0.2	*ND*

nd not detected; *ND* not determined; *r* residual activity;

[1)] Ratio of the initial activity of the variant to the parent type (Ai_v/Ai_p).

[2)] Ratio of the relative activity to the initial activity of the variant (v), normalized to the parent type (p) - $(Ar/Ai)_v/(Ar/Ai)_p$.

[3)] 100% of activity after 3.5 h of incubation at 4ºC;

[4)] Initial activity and stability relative to variant 21G11

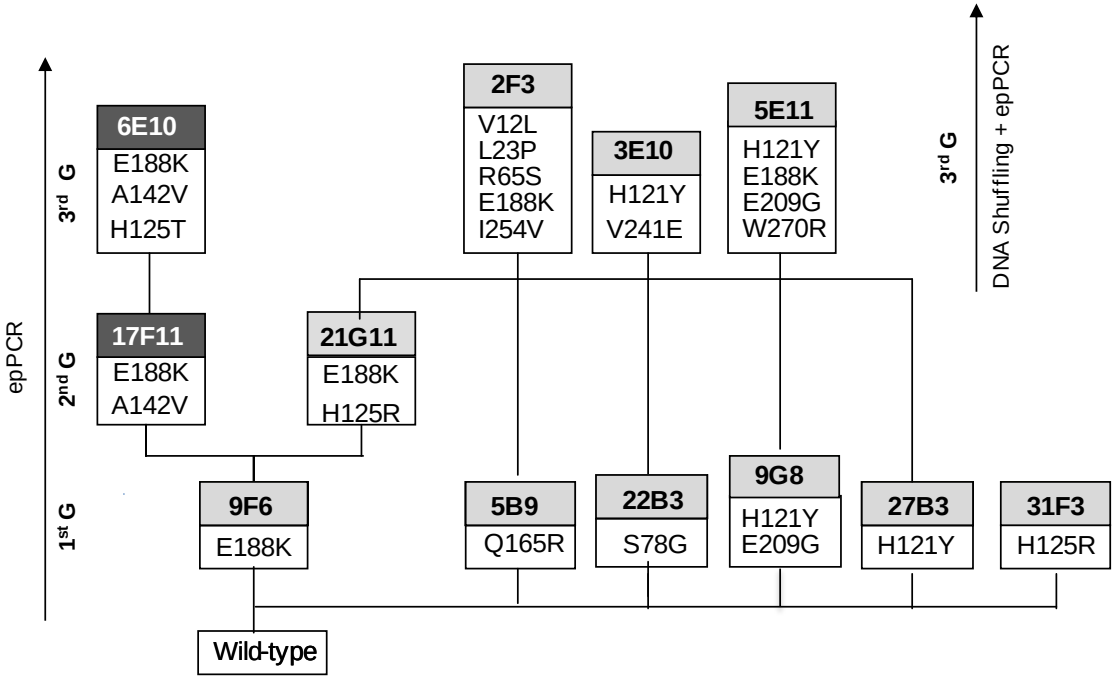

Figure 4 – Lineage of PpDyP variants generated in this study. The mutants with higher activity for ABTS are in light grey and black letters and the mutants with higher activity for DMP are in dark grey and white letters.

In the 2nd generation, a total of 1928 clones were screened (Figure 5A) and 9 variants were identified with improvements in the initial activity and/or in stability and re-screened for ABTS and DMP to rule out false positives (Figure 5B).

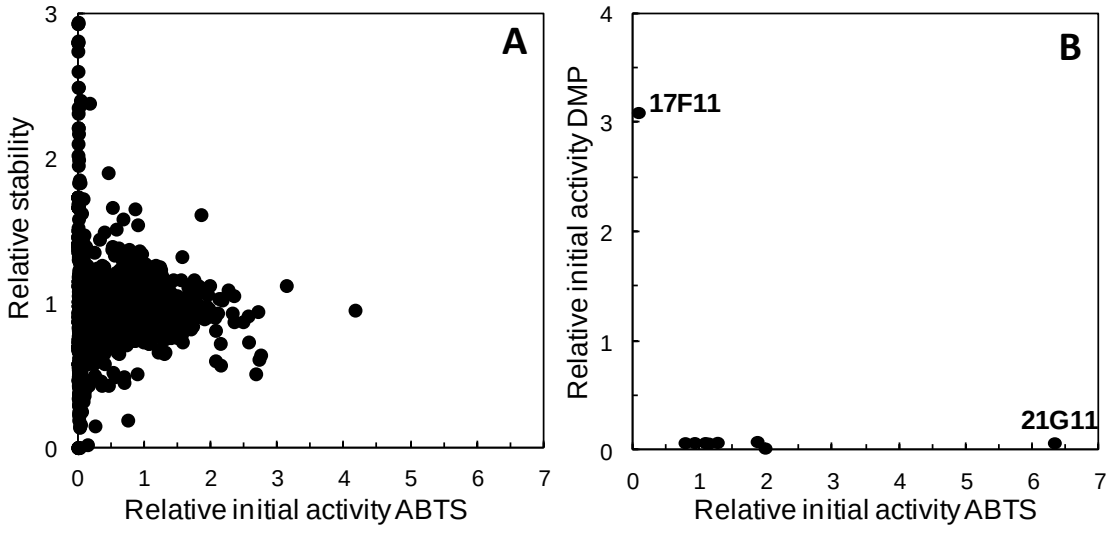

Figure 5 – Directed evolution landscape for the second generation mutant library. **A –** Initial activity vs stability of 1928 clones screened relative to the 9F6. Stability is measured by the ratio of residual activity following incubation at 4°C for 2.5 h to initial activity. **B –** Re-screening of the best mutants identified in the second generation. Initial activity using ABTS as substrate vs initial activity using DMP as substrate.

Two variants were selected: the 21G11 variant showing a 6-fold higher activity for ABTS, while maintaining a similar stability when compared with the parent (9F6) (Figure 5B and Table 3) and 17F11 variant showing 3-fold higher activity relative to the parent (9F6) using DMP as substrate (Table 3). Both variants shared the mutation E188K from the parent and while the 17F11 acquired the additional mutation A142V, 21G11 acquired mutation H125R.

Variant 17F11 was therefore chosen as parent for the 3rd generation with the aim of improving activity for the phenolic DMP. First we have validated the screening using this DMP was performed; 17F11 variant was overproduced in 96-well plates, cells were disrupted and crude extracts were used for activity measurements. A CV ~ 45% was obtained for the 17F11 variant. This high CV was only observed for the enzymatic activity while the OD_{600nm} of cell cultures and protein concentration of crude extracts show CVs below 20%, suggesting that mutation A142V introduces most likely a considerable variation in the expression/transcription of the gene or translation of RNA to proteins. After several attempts of optimization and despite the risks of having a very high CV, it was decided to move forward using this variant as the parent for the next round of directed evolution.

In the 3rd generation of epPCR using 17F11 as parent, a total of 1793 clones were screened (Figure 6A) and 5 variants were identified with improvements in initial activity and/or in stability in relation to the parental enzyme. Their re-screening allowed identifying a positive hit, the 6E10 variant with the following mutations: E188K, A142V, H125T (Figure 6B).

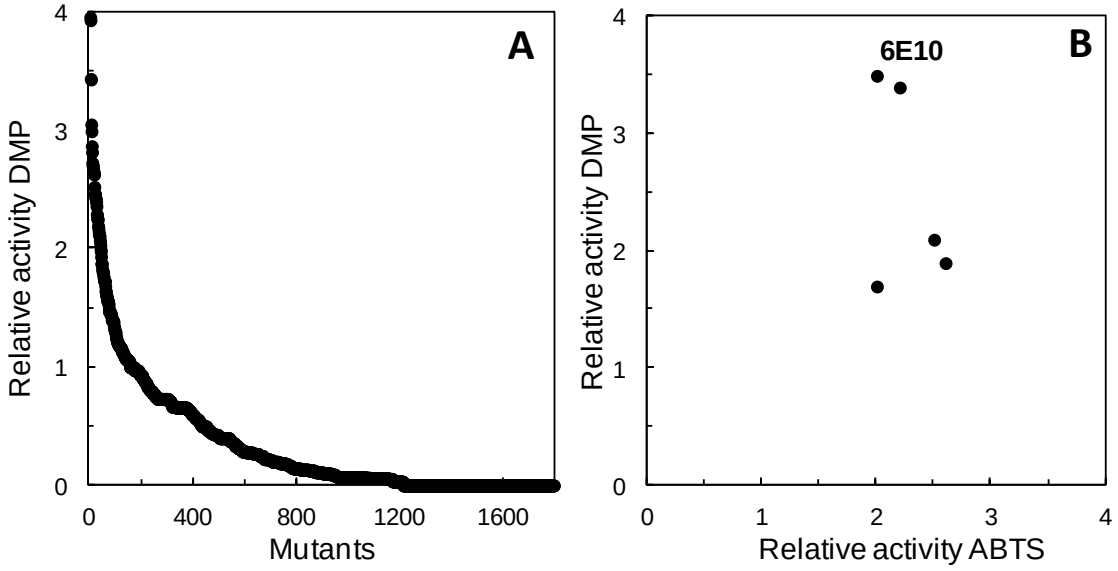

Figure 6 – Directed evolution landscape for the third generation mutant library. **A –** Initial activity of 1793 clones screened relative to 17F11. **B –** Re-screening of the best variants identified. Initial activity using ABTS as substrate vs initial activity using DMP as substrate.

This variant showed 3.5- and 2-fold higher activity for DMP and ABTS, respectively, when compared to the parental enzyme (17F11) and was selected as parent for the 4th generation (Figure 4, Table 3). Moreover, it seems to be more stable than the parent since it did not lose activity after 3.5 h at 4ºC.

To further validate the screening, the 6E10 variant was overproduced in 96-well plates, cells were disrupted and crude extracts were used for activity measurement using DMP as substrate. The CV for the enzymatic activity was 28%, showing a drop of ~ 20% when compared to the one obtained for the parental enzyme (17F11).

In the 4th generation using 6E10 as parent, a total of 1920 clones were screened. However, a high number of inactive variants (~ 70%) were detected and none of the variants screened showed higher activity than the parental enzyme. In fact, the DNA sequence analysis of several variants revealed that they all had the same genotype of the parental variant 6E10. Therefore, new libraries were created by epPCR with a higher concentration of $MnCl_2$, 0.02 mM, since it is more likely to find variants with improved or novel functions with a higher error-rate (Drummond *et al.*, 2005). As expected, these conditions resulted in a higher number of inactive variants (~ 85%) however it was not possible to detect any improved variants. Thus, it was decided to screen the libraries for thermostable hits since more robust enzymes will accept with easiness the introduction of new mutations that tend to be destabilizing due to the well-known trade-off between high activity and high stability (Jaenicke and Bohm, 1998). For the set-up of the thermostability assays a time of incubation of 45 min at 50°C was selected using the 6E10 variant based on conditions that resulted in a residual activity of about one-third of the initial activity. Therefore, in a near future libraries of 3rd and 4th generation will be re-screened in an attempt to find more thermostable variants that will allow continuing the evolution of PpDyP towards an improved activity for phenolic substrates.

3.1.5.2 Towards improved catalytic efficiency for ABTS

As a result of the screening of the 2nd generation variant 21G11 was selected showing 6-fold higher activity for ABTS (Table 3, Figure 5B). The mutation acquired by this variant, H125R, was already present in variant 31F3 from the 1st generation (Figure 4). The observation of this synergistic effect between mutation E188K and H125R led us to follow a recombination/epPCR approach using variant 21G11 and variants 5B9, 9G8, 22B3 and 27B3 identified in the 1st generation (Figure 4); genes from these variants were amplified by epPCR in the presence of 0.01 mM $MnCl_2$, pooled and digested with DNase I during a period of time that lead to a smear of DNA fragments with sizes below 250 bp in agarose gels. These fragments were submitted to a “progressive hybridization” PCR program involving seven hybridization steps to force low homology recombination. A large smear of high molecular

weight DNA was formed. A second PCR step, involving primers located on the cDNA flanking regions, was performed and amplification of a well-defined band ~ 1200 bp was observed (Figure 7).

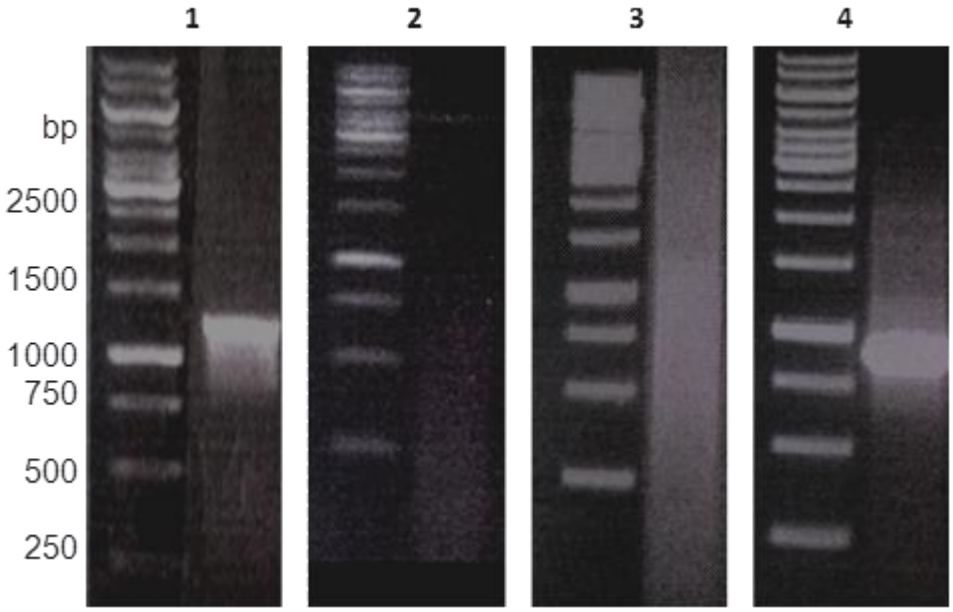

Figure 7 - Steps of DNA shuffling performed in the 3rd generation. **1 –** DNA amplification of the gene by epPCR. **2 -** Digestion with DNase I. **3 -** Reassembly of DNA fragments. **4 –** Amplification of full-lenght sequence.

This PCR product was cloned and used to transform *E. coli* KRX cells and a total of 648 variants were screened. Nine variants were identified with improvements in initial activity using ABTS as substrate (Figure 8A) and re-screened to rule out false positives (Figure 8B).

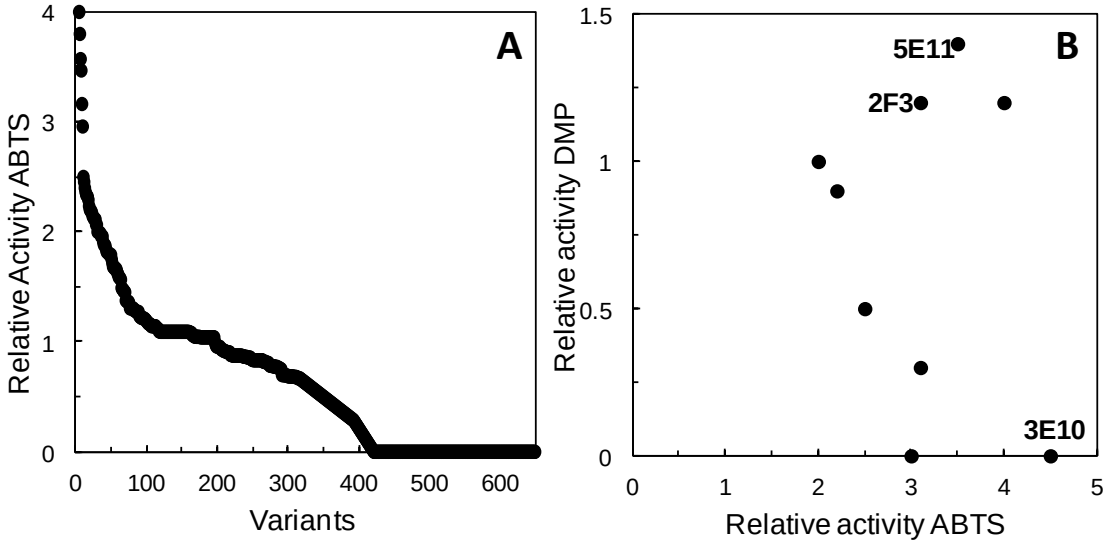

Figure 8 – Directed evolution landscape for the third generation mutant library, constructed by DNA shuffling and epPCR. **A –** Initial activity of 648 clones screened relative to 21G11. **B –** Re-screening of the best variants identified. Initial activity using DMP as substrate vs initial activity using ABTS as substrate.

Three hit variants were selected, 2F3, 3E10 and 5E11, showing an improvement in initial activity of around 3- to 4.5-fold when compared to the 21G11 variant (Table 3).

The DNA sequence analysis of these variants revealed the mutations V12L, L23P, R65S, E188K, I254V in the variant 2F3, mutations H121Y, V241E in the variant 3E10 and mutations H121Y, E188K, E209G, W270R in the variant 5E11. These results show: (1) that variant 5E11 resulted from a simple recombination between the genes from 21G11 and 9G8 variants while (2) 2F3 and 3E10 variants acquired new mutations during the epPCR step. Interestingly, variant 3E10 acquired four mutations in contrast to the average of one amino acid substitution observed during the PpDyP evolution (Figure 4, Table 3). Future work may include screening of more variants from this library or construction of a new library using DNA shuffling approach without the introduction of new mutations by epPCR.

3.2 Spectroscopic and Biochemical Characterization of PpDyP Wild-type and Variants

3.2.1 Spectroscopic characterization

The *ppDyP* genes from Wt and variants 9F6, 21G11, 17G11 and 6E10 were cloned into the expressing vector pET-21a(+) and subsequently transformed into *E. coli* Tuner strain. SDS-PAGE analysis of crude extracts from the recombinant cells revealed that the addition of IPTG to the culture medium resulted in the accumulation of an additional band at ~ 32 kDa. The recombinant enzymes were purified from crude extracts using two chromatographic steps to apparent homogeneity as determined by SDS-PAGE analysis (Figure 9), with purification yields of 46, 73, 47, 48 and 30% for PpDyP Wt and variants 9F6, 21G11, 17F11 and 6E10, respectively. Variants 21G11 (2nd G) and 6E10 (3rd G) exhibited a 2.6- and 2.0-fold increase in the enzyme production (14.5 and 11.5 mg/L, respectively) when compared with the Wt enzyme (5.5 mg/L). Interestingly, both variants acquired a mutation in the residue His125, suggesting that this position is a hot-spot to enhance the PpDyP production.

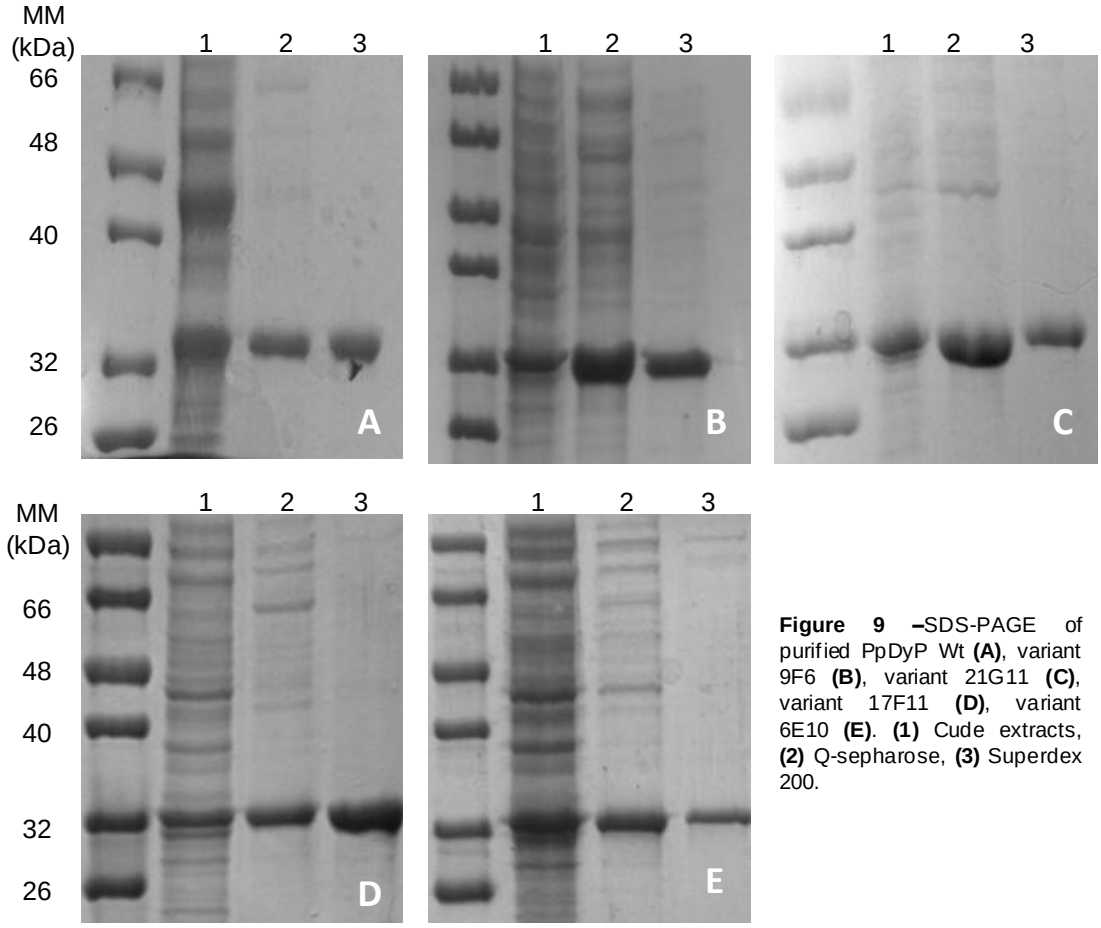

Figure 9 –SDS-PAGE of purified PpDyP Wt **(A)**, variant 9F6 **(B)**, variant 21G11 **(C)**, variant 17F11 **(D)**, variant 6E10 **(E)**. **(1)** Cude extracts, **(2)** Q-sepharose, **(3)** Superdex 200.

The overall electronic absorption features of PpDyp variants as assessed by UV-visible spectra reveal the characteristic Soret band at ~ 400 nm, Q bands at ~ 502 and 545 nm, and a charge transfer band at ~ 630 nm (Figure 10), as observed in Wt enzyme (Santos *et al.*, 2014).

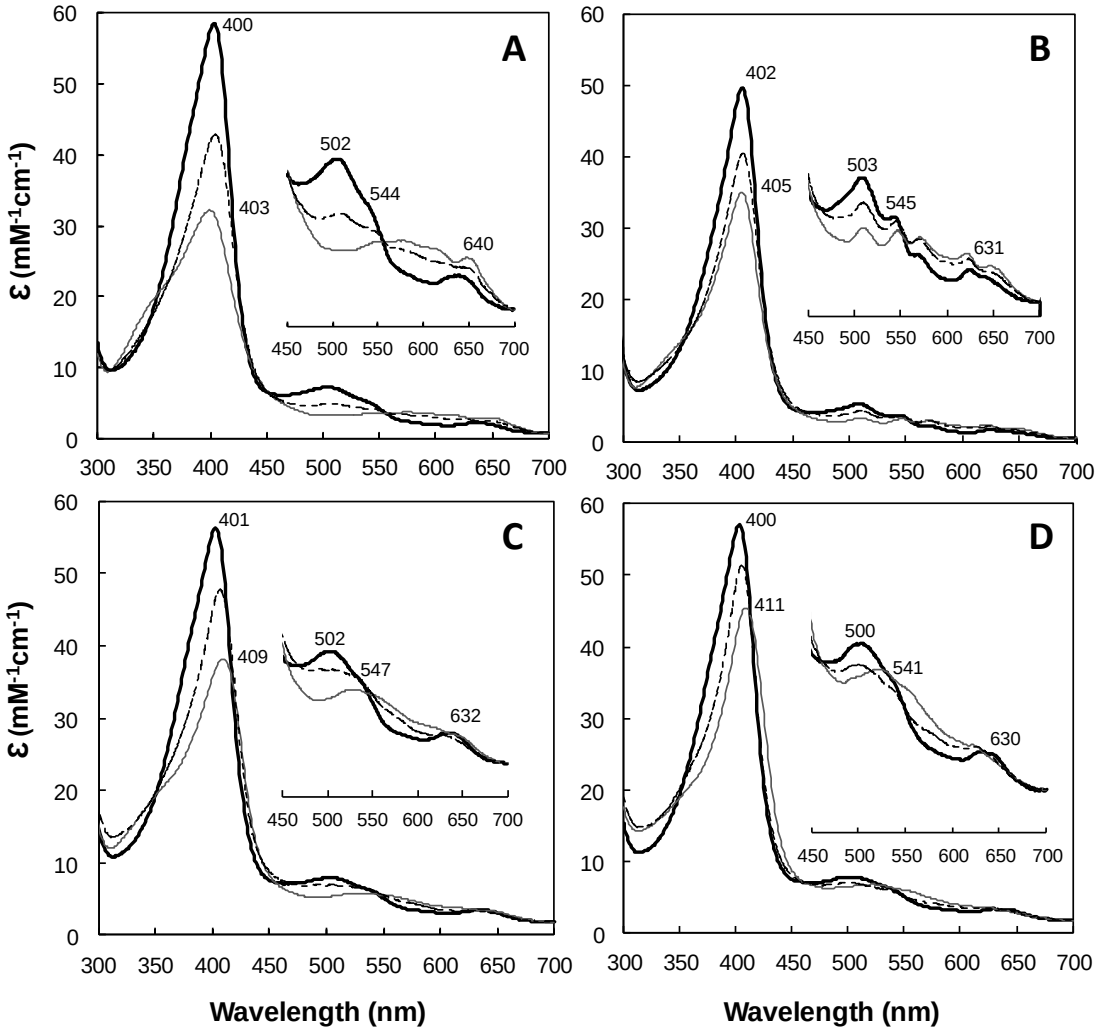

Figure 10 - UV-vis spectra of PpDyP variants **(A)** 9F6, **(B)** 21G11, **(C)** 17F11 and **(D)** 6E10. Resting state (black solid line), immediately after the addition of 1 equivalent of H_2O_2 (gray solid line) and after 1 hour (dashed line).

Heme *b* content was estimated by the pyridine ferrohemochrome method. Spectra of PpDyP Wt and variants showed absorption peaks corresponding to the Soret Band at ~ 419 nm and to the Q band at ~ 522 nm, characteristics of iron protoporphyrin IX. Heme *b* content for 9F6, 21G11, 17F11 and 6E10 variants was estimated to be 0.9 ± 0.1, 0.8 ± 0.1, 0.9 ± 0.1 and 0.9 ± 0.08 mol per mole of protein, respectively, similarly to the Wt (1 ± 0.07 mol per mole of protein).

All heme peroxidases require hydrogen peroxide or other hydroperoxides to activate the heme cofactor yielding the so-called compound I intermediate in a common catalytic cycle (Hiner *et al.*, 2002). Compound I contains a reactive Fe^{4+} oxo complex with a cation radical at the porphyrin ring, formed by two-electron oxidation of the Fe^{3+}-containing heme of the resting

enzyme. The formation of an intermediate with spectral features of Compound I (decrease in intensity of a Soret band, disappearance of Q bands and appearance of a band ~ 550-600 nm) was observed upon addition of 1 equivalents of hydrogen peroxide to all variants (Figure 10). After 1 h variants returned to its ferric initial resting state, similarly to the Wt (Santos *et al.*, 2014).

3.2.2 Kinetic properties

The overall pH activity profile of PpDyP Wt and variants was determined using DMP and ABTS as substrates in the presence of H_2O_2 (Figure 11A and B). Variants 17F11 (2nd G) and 6E10 (3rd G) revealed different pH optima values when compared to Wt (pH_{opt} = 4.3). Both variants increase the pH optima by 4.1 and 1.1 units to pH 8.4 and 5.4 for DMP and ABTS, respectively. The mutation A142V, introduced in the 17F11 gene (2nd G), seems to be the responsible for this up-shift in the optimal pH. Recently, the function of the distal residues D132, R214 and N136 were studied by combining site-directed mutagenesis and spectroscopic, kinetic and electrochemical studies. It was observed that the N136L mutant shows maximal activity for ABTS at around pH 5.6. The mutation A142V is located 7.5 Å from the catalytic residue N136 and probably introduces some structural changes, inducing a variation in the pH profile that is presently unclear (Mendes *et al.*, submitted, 2014).

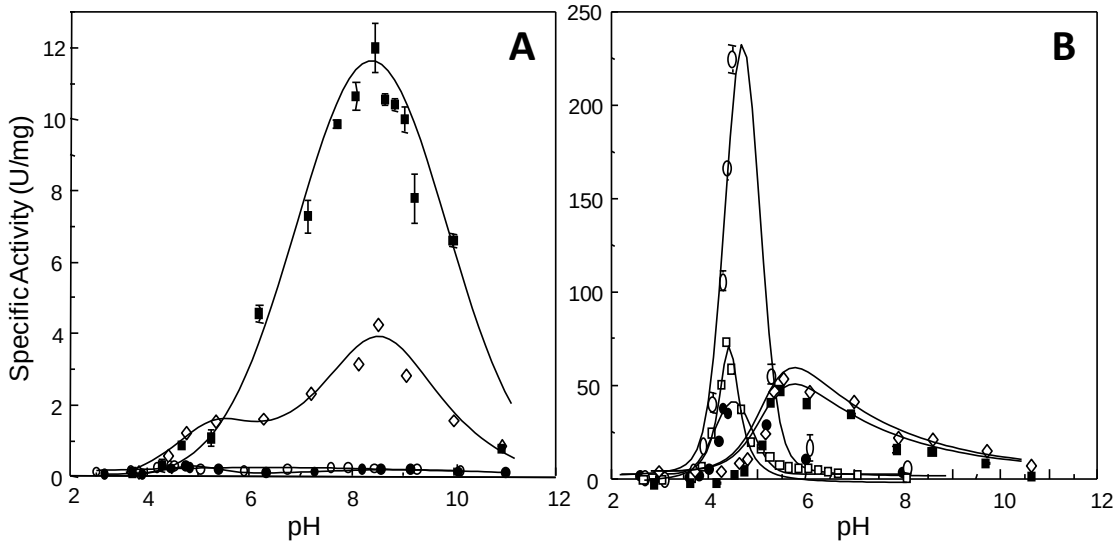

Figure 11 - pH activity profile using **(A)** DMP and **(B)** ABTS as substrates of PpDyP wild-type (●) and variants, 9F6 (○), 21G11 (□),17F11 (◊) and 6E10 (■).

3.2.2.1 Towards improved catalytic efficiency for DMP

The catalytic properties of PpDyP Wt and 9F6, 17F11 and 6E10 variants were probed by stead-state kinetics for reduction of H_2O_2 and oxidation of several substrates including ABTS, phenolics compounds (DMP and guaiacol), and the metal ions Mn^{2+} and Fe^{2+} (Table 4).

Table 4 – Steady-state apparent constants of purified PpDyP and 9F6, 17F11 and 6E10 variants.

K_m (µM)				
	Wt	**9F6**	**17F11**	**6E10**
H_2O_2 (ABTS)	79 ± 5	60 ± 16	100 ± 14	34 ± 7
ABTS	2494 ± 276	250 ± 56	788 ± 90	720 ± 88
DMP	120 ± 21	78 ± 13	42 ± 4	58 ± 6
Guaiacol	32 ± 6	ND	61 ± 9	36 ± 0.4
Mn^{2+}	272 ± 54	152 ± 36	334 ± 66	284 ± 43
Fe^{2+}	-	131 ± 51	102 ± 15	300 ± 63
V_{max} (U/mg)				
	Wt	**9F6**	**17F11**	**6E10**
H_2O_2 (ABTS)	27 ± 1.2	131 ± 10	16 ± 2	27 ± 1.1
ABTS	80 ± 2.5	204 ± 13	65 ± 6	83 ± 9
DMP	0.15 ± 0.01	0.17 ± 0.01	7 ± 0.2	12 ± 3
Guaiacol	0.1 ± 0.003	0.07 ± 0.01	0.7 ± 0.03	1.4 ± 0.03
Mn^{2+}	8 ± 0.9	11 ± 0.9	7 ± 0.6	8 ± 1.3
Fe^{2+}	0.5 ±0.05	1.2 ± 0.1	1 ± 0.05	1.2 ± 0.1
K_{cat}/K_m ($M^{-1}s^{-1}$)				
	Wt	**9F6**	**17F11**	**6E10**
H_2O_2 (ABTS)	1.8×10^5	1.1×10^6	0.8×10^5	4×10^5
ABTS	1.6×10^4	4.2×10^5	4.3×10^4	6×10^4
DMP	4×10^2	10×10^2	8×10^4	10×10^4
Guaiacol	1.6×10^3	ND	0.6×10^4	2×10^4
Mn^{2+}	15×10^3	38×10^3	11×10^3	15×10^3
Fe^{2+}	-	4.8×10^3	5.1×10^3	2.1×10^3

The analysis of the kinetic data of PpDyP Wt and variants (Table 4) reveals that 9F6 variant (from the first generation (1st G)) shows an improvement of 1 order of magnitude for the specificity (k_{cat}/K_m) of ABTS when compared to the Wt as a result of a ~ 10 times lower K_m and 2.5 times higher V_{max} (204 U/mg vs 80 U/mg). Moreover, an improvement of 1 order of magnitude in the specificity for hydrogen peroxide as a result of ~ 5 times higher V_{max} was also observed. This variant also revealed an improvement of 2.4-fold in the rate of Fe^{2+} oxidation. The inhibitory effect of high concentrations of Fe^{2+} over the enzyme activity was similar to the one observed in the Wt enzyme (Santos *et al.*, 2014). This variant, as expected, does not show major differences in the catalytic constants for the oxidation of phenolic compounds when compared to the Wt enzyme.

Variants 17F11 (2nd G) and 6E10 (3rd G) show an improvement of ~ 2 orders of magnitude for DMP specificity as a result of a ~ 3- and 2-fold lower K_m and ~ 45- and 80-fold higher V_{max}, respectively when compared to the PpDyP Wt.. For the other phenolic compound tested, guaiacol, the improvement was not so pronounced however, it was also observed a 1 order of

magnitude increase in the specificity, resulting in a ~ 10 times higher V_{max}. The analysis of the kinetic data for H_2O_2 and ABTS shows that introduction of A142V mutation results in a recede for ABTS oxidation since variant 17F11 shows similar specificities to those of the Wt.

The mutations introduced during the molecular evolution did not altered the inhibitory effect of hydrogen peroxide over the PpDyP activity and all variant enzymes showed a K_i of ~ 0.4 mM, as previously observed for the Wt enzyme (Santos *et al.*, 2014).

3.2.2.2 Towards improved catalytic efficiency for ABTS

The kinetic properties of the variant 21G11 (2nd G) selected using ABTS as substrate are very similar to the parental enzyme (9F6) showing however an improvement of 1 order of magnitude for the specificity (k_{cat}/K_m) of ABTS when compared to the Wt as a result of a ~ 10 times lower K_m (Table 4 and 5). These results suggest that mutation H125R acquired in this generation led to an increase of the total amount of active enzyme, rather than a more active variant, as suggested previously.

Table 5 – Steady-state apparent constants of purified 21G11 variant.

	K_m (µM)	V_{max} (U/mg)	K_{cat}/K_m ($M^{-1}.s^{-1}$)
H_2O_2 (ABTS)	52 ± 13	154 ± 13	1.5×10^6
ABTS	228 ± 57	82 ± 5	1.8×10^5
DMP	34 ± 10	0.04 ± 0.003	6×10^2
Guaiacol	32 ± 6	0.08 ± 0.003	1.2×10^3
Mn^{2+}	161 ± 29	12.3 ± 1.6	40×10^3
Fe^{2+}	136 ± 37	1.3 ± 0.08	4.9×10^3

3.2.3 Kinetic Stability of PpDyP variants

Considering the known potential of DyPs for applications in the areas of transformation of lignin-related substrates, we have studied the kinetic stability of the enzymes (Figure 12) that quantifies the amount of enzyme that loses activity irreversibly during incubation at a certain temperature.

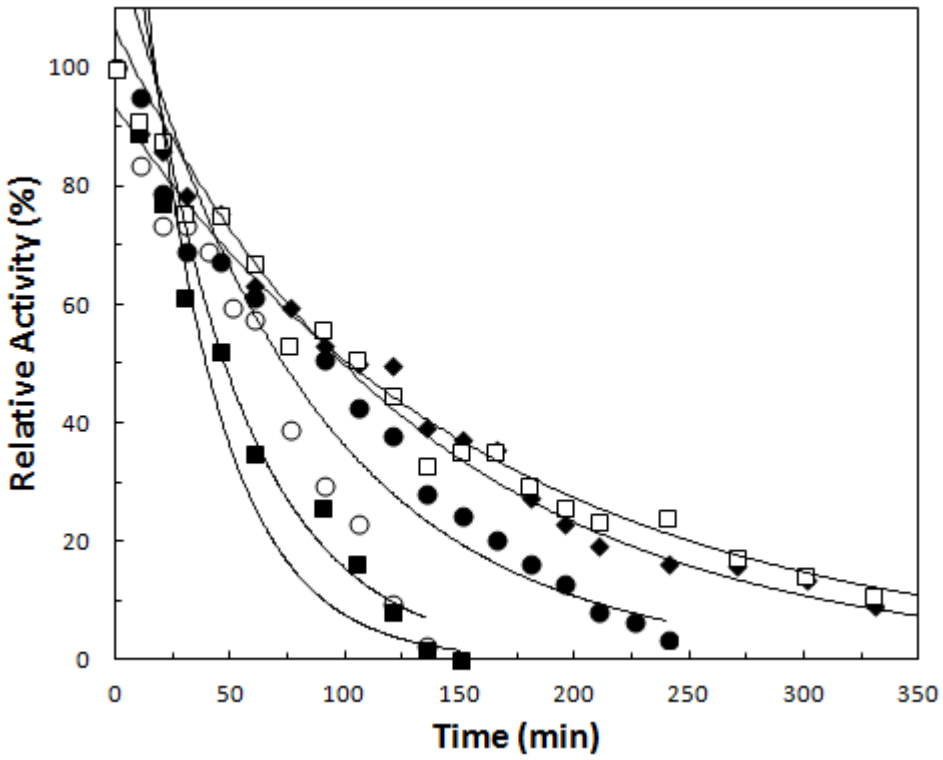

Figure 12 – Kinetic stability of PpDyP (♦), and variants 9F6 (○), 21G11 (●), 17F11 (■) and 6E10 (□) at 40ºC at pH 7.6.

The kinetic thermal denaturation profiles indicate that the most active variant from the 1st generation (9F6) showed a lower half-life inactivation at 40^0 C and pH 7.6 (52 ± 8 min^{-1}), when compared with the Wt (110 ± 17 min^{-1}), revealing a trade-off between high activity and high stability (Jaenicke and Bohm, 1998). Interestingly, both variants that acquired a mutation in the position His125 (the 21G11 from the 2nd generation and the 6E10 from the 3rd generation) showed an increase in kinetic stability when compared with the 9F6 variant and half-lives inactivation of 71 ± 11 min^{-1} and 114 ± 12 min^{-1}, similar to that of the Wt. Thus, substitution of His125 induced an increase not only in the protein production but also in protein stabilization.

3.3 Structural analysis of mutations

PpDyP is a homotetramer and its model structure was reasonably modeled using template sequences from the bacterial structure from crystal structures of BtDyP (Zubieta *et al.*, 2007b) and TryA (Zubieta *et al.*, 2007a). The overall fold shows the typical ferrodoxin-like fold with the heme cofactor sandwiched between distal and proximal sides (Santos *et al.*, 2014). The distal side is composed by an aspartate, an asparagine and an arginine and the proximal side contains a histidine and an aspartate residues.

From the three modified positions during the evolution process, two (E188 and H125) are located in loops on the surface of the enzyme and one (A142) in an α-helix on the interface of the enzyme. The three positions are situated in the second shell of the active site residues (Figure 13).

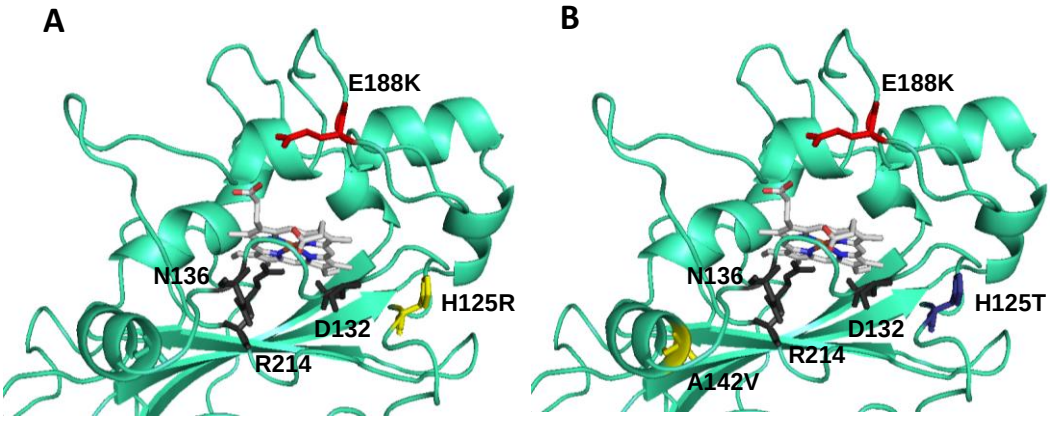

Figure 13 – Structural mapping of key amino acids for protein activity and stability/expression in PpDyP model structure. **A** - 21G11 and **B** - 6E10 variants. Mutation from 1st generation is in red, mutations from 2nd generation are in yellow and the mutation from 3rd generation is in dark blue. The catalytic residues are in dark gray.

The variant with the best performance for ABTS oxidation and H_2O_2 reduction, 21G11 (Figure 8A), share the mutation E188K introduced in the 1st generation with the variant 6E10 (Figure 8B). The negatively charged residue Glu188 is located around 12 Å from the catalytic distal residues. The introduction of a positively charged residue in this position, Lys seems to facilitate the binding of the negatively charged oxidizing substrate ABTS and also induces conformational changes in the active site, which increases the rate for ABTS and metals oxidation and H_2O_2 reduction. Both variants, 21G11 and 6E10, also acquired other mutation in the same position, His125, located 5 Å from the catalytic residue Asp132 and as discussed above the substitution for either an arginine or a threonine enhances the stability of the enzyme, improving the protein production and kinetic stability. The variant 6E10 accumulated one more mutation, A142V, located 8 Å from the catalytic residue Asn136 and to a large extent responsible for the increased of phenolic compounds oxidation rate.

4. Conclusions

Directed evolution, using epPCR approach has proven to be an important tool for improving the catalytic properties and protein production of PpDyP, by allowing the accumulation of one amino acid change in each generation. The mutation rate of only one substitution per gene in each generation allowed us to better understand the role of each mutation.

After 3 rounds of evolution using epPCR and DNA shuffling we identified 12 hits with improved catalytic activity. Through the analysis of DNA sequences and kinetic studies the mutation E188K seemed to be responsible an improvement of 25- and 6-fold for ABTS oxidation and H_2O_2 reduction specificity, respectively. The mutation A142V revealed to be responsible for a 250-fold enhancement of the specificity for the phenolic compound DMP. It was also observed that position His125 is a hot-spot to enhance the stability of the enzyme, improving both the protein production and kinetic stability.

It was also observed that it is difficult to improve simultaneously the activity and the stability of the enzyme due to the trade-off between high activity and high stability.

In the future it would be interesting to perform a screening for stability in the libraries of the 3rd and 4th generation, in an attempt to find a more stable variant, and then continuing the screening for variants with higher activity for phenolic compounds. It would be also important to perform a new library, with variant 21G11 and the variants from 1st generation, using DNA shuffling approach to understand if the mutations identified in the first generation have a synergistic effect.

5. References

Berry, E.A., Trumpower, B.L., 1987. Simultaneous determination of hemes a, b, and c from pyridine hemochrome spectra. Anal Biochem 161, 1-15.

Bloom, J.D., Meyer, M.M., Meinhold, P., Otey, C.R., MacMillan, D., Arnold, F.H., 2005. Evolving strategies for enzyme engineering. Curr Opin Struct Biol 15, 447-452.

Brakmann, S., 2001. Discovery of superior enzymes by directed molecular evolution. Chembiochem 2, 865-871.

Brissos, V., Goncalves, N., Melo, E.P., Martins, L.O., 2014. Improving kinetic or thermodynamic stability of an azoreductase by directed evolution. PLoS One 9, e87209.

Bugg, T.D., Ahmad, M., Hardiman, E.M., Singh, R., 2011. The emerging role for bacteria in lignin degradation and bio-product formation. Curr Opin Biotechnol 22, 394-400.

Cirino, P.C., Mayer, K.M., Umeno, D., 2003. Generating mutant libraries using error-prone PCR. Methods Mol Biol 231, 3-9.

Colpa, D.I., Fraaije, M.W., van Bloois, E., 2014. DyP-type peroxidases: a promising and versatile class of enzymes. J Ind Microbiol Biotechnol 41, 1-7.

Dougherty, M.J., Arnold, F.H., 2009. Directed evolution: new parts and optimized function. Curr Opin Biotechnol 20, 486-491.

Drummond, D.A., Iverson, B.L., Georgiou, G., Arnold, F.H., 2005. Why high-error-rate random mutagenesis libraries are enriched in functional and improved proteins. J Mol Biol 350, 806-816.

Garcia-Ruiz, E., Gonzalez-Perez, D., Ruiz-Duenas, F.J., Martinez, A.T., Alcalde, M., 2012. Directed evolution of a temperature-, peroxide- and alkaline pH-tolerant versatile peroxidase. Biochem J 441, 487-498.

Garcia-Ruiz, E., Mate, D., Ballesteros, A., Martinez, A.T., Alcalde, M., 2010. Evolving thermostability in mutant libraries of ligninolytic oxidoreductases expressed in yeast. Microb Cell Fact 9, 17.

Georgescu, R., Bandara, G., Sun, L., 2003. Saturation mutagenesis. Methods Mol Biol 231, 75-83.

Hiner, A.N., Raven, E.L., Thorneley, R.N., Garcia-Canovas, F., Rodriguez-Lopez, J.N., 2002. Mechanisms of compound I formation in heme peroxidases. J Inorg Biochem 91, 27-34.

Hofrichter, M., Ullrich, R., Pecyna, M.J., Liers, C., Lundell, T., 2010. New and classic families of secreted fungal heme peroxidases. Appl Microbiol Biotechnol 87, 871-897.

Jaenicke, R., Bohm, G., 1998. The stability of proteins in extreme environments. Curr Opin Struct Biol 8, 738-748.

Johnson, B.H., Hecht, M.H., 1994. Recombinant proteins can be isolated from E. coli cells by repeated cycles of freezing and thawing. Biotechnology (N Y) 12, 1357-1360.

Jongbloed, J.D., Grieger, U., Antelmann, H., Hecker, M., Nijland, R., Bron, S., van Dijl, J.M., 2004. Two minimal Tat translocases in Bacillus. Mol Microbiol 54, 1319-1325.

Kim, S.J., Shoda, M., 1999. Purification and characterization of a novel peroxidase from Geotrichum candidum dec 1 involved in decolorization of dyes. Appl Environ Microbiol 65, 1029-1035.

Kuan, I.C., Johnson, K.A., Tien, M., 1993. Kinetic analysis of manganese peroxidase. The reaction with manganese complexes. J Biol Chem 268, 20064-20070.

Kuchner, O., Arnold, F.H., 1997. Directed evolution of enzyme catalysts. Trends Biotechnol 15, 523-530.

Lin, Z., Thorsen, T., Arnold, F.H., 1999. Functional expression of horseradish peroxidase in E. coli by directed evolution. Biotechnol Prog 15, 467-471.

Liu, X., Du, Q., Wang, Z., Zhu, D., Huang, Y., Li, N., Wei, T., Xu, S., Gu, L., 2011. Crystal structure and biochemical features of EfeB/YcdB from Escherichia coli O157: ASP235 plays divergent roles in different enzyme-catalyzed processes. J Biol Chem 286, 14922-14931.

Martinez, A.T., Ruiz-Duenas, F.J., Martinez, M.J., Del Rio, J.C., Gutierrez, A., 2009. Enzymatic delignification of plant cell wall: from nature to mill. Curr Opin Biotechnol 20, 348-357.

Mendes, S., Brissos, V., Gabriel, A., Catarino, T., Todorovic, S., Martins, L.O., submitted, 2014. An integrated view of redox and catalytic properties of B-type 1 PpDyP from Pseudomonas putida MET94 and its distal variants. Arch. Biochem. Biophys.

Molina-Espeja, P., Garcia-Ruiz, E., Gonzalez-Perez, D., Ullrich, R., Hofrichter, M., Alcalde, M., 2014. Directed evolution of unspecific peroxygenase from Agrocybe aegerita. Appl Environ Microbiol 80, 3496-3507.

Morawski, B., Lin, Z., Cirino, P., Joo, H., Bandara, G., Arnold, F.H., 2000. Functional expression of horseradish peroxidase in Saccharomyces cerevisiae and Pichia pastoris. Protein Eng 13, 377-384.

Reetz, M.T., Kahakeaw, D., Lohmer, R., 2008. Addressing the numbers problem in directed evolution. Chembiochem 9, 1797-1804.

Rodriguez-Couto, S., 2009. Enzymatic biotransformation of synthetic dyes. Curr Drug Metab 10, 1048-1054.

Romero, P.A., Arnold, F.H., 2009. Exploring protein fitness landscapes by directed evolution. Nat Rev Mol Cell Biol 10, 866-876.

Salazar, O., Sun, L., 2003. Evaluating a screen and analysis of mutant libraries. Methods Mol Biol 230, 85-97.

Santos, A., Mendes, S., Brissos, V., Martins, L.O., 2014. New dye-decolorizing peroxidases from Bacillus subtilis and Pseudomonas putida MET94: towards biotechnological applications. Appl Microbiol Biotechnol 98, 2053-2065.

Scheibner, M., Hulsdau, B., Zelena, K., Nimtz, M., de Boer, L., Berger, R.G., Zorn, H., 2008. Novel peroxidases of Marasmius scorodonius degrade beta-carotene. Appl Microbiol Biotechnol 77, 1241-1250.

Singh, R., Grigg, J.C., Armstrong, Z., Murphy, M.E., Eltis, L.D., 2012. Distal heme pocket residues of B-type dye-decolorizing peroxidase: arginine but not aspartate is essential for peroxidase activity. J Biol Chem 287, 10623-10630.

Strittmatter, E., Liers, C., Ullrich, R., Wachter, S., Hofrichter, M., Plattner, D.A., Piontek, K., 2013. First crystal structure of a fungal high-redox potential dye-decolorizing peroxidase: substrate interaction sites and long-range electron transfer. J Biol Chem 288, 4095-4102.

Sugano, Y., 2009. DyP-type peroxidases comprise a novel heme peroxidase family. Cell Mol Life Sci 66, 1387-1403.

Tracewell, C.A., Arnold, F.H., 2009. Directed enzyme evolution: climbing fitness peaks one amino acid at a time. Curr Opin Chem Biol 13, 3-9.

Welinder, K.G., Mauro, J.M., Norskov-Lauritsen, L., 1992. Structure of plant and fungal peroxidases. Biochem Soc Trans 20, 337-340.

Yoshida, T., Tsuge, H., Konno, H., Hisabori, T., Sugano, Y., 2011. The catalytic mechanism of dye-decolorizing peroxidase DyP may require the swinging movement of an aspartic acid residue. FEBS J 278, 2387-2394.

Zederbauer, M., Furtmuller, P.G., Brogioni, S., Jakopitsch, C., Smulevich, G., Obinger, C., 2007. Heme to protein linkages in mammalian peroxidases: impact on spectroscopic, redox and catalytic properties. Nat Prod Rep 24, 571-584.

Zubieta, C., Joseph, R., Krishna, S.S., McMullan, D., Kapoor, M., Axelrod, H.L., Miller, M.D., Abdubek, P., Acosta, C., Astakhova, T., Carlton, D., Chiu, H.J., Clayton, T., Deller, M.C., Duan, L., Elias, Y., Elsliger, M.A., Feuerhelm, J., Grzechnik, S.K., Hale, J., Han, G.W., Jaroszewski, L., Jin, K.K., Klock, H.E., Knuth, M.W., Kozbial, P., Kumar, A., Marciano, D., Morse, A.T., Murphy, K.D., Nigoghossian, E., Okach, L., Oommachen, S., Reyes, R., Rife, C.L., Schimmel, P., Trout, C.V., van den Bedem, H., Weekes, D., White, A., Xu, Q., Hodgson, K.O., Wooley, J., Deacon, A.M., Godzik, A., Lesley, S.A., Wilson, I.A., 2007a. Identification and structural characterization of heme binding in a novel dye-decolorizing peroxidase, TyrA. Proteins 69, 234-243.

Zubieta, C., Krishna, S.S., Kapoor, M., Kozbial, P., McMullan, D., Axelrod, H.L., Miller, M.D., Abdubek, P., Ambing, E., Astakhova, T., Carlton, D., Chiu, H.J., Clayton, T., Deller, M.C., Duan, L., Elsliger, M.A., Feuerhelm, J., Grzechnik, S.K., Hale, J., Hampton, E., Han, G.W., Jaroszewski, L., Jin, K.K., Klock, H.E., Knuth, M.W., Kumar, A., Marciano, D., Morse, A.T., Nigoghossian, E., Okach, L., Oommachen, S., Reyes, R., Rife, C.L., Schimmel, P., van den Bedem, H., Weekes, D., White, A., Xu, Q., Hodgson, K.O., Wooley, J., Deacon, A.M., Godzik, A., Lesley, S.A., Wilson, I.A., 2007b. Crystal structures of two novel dye-decolorizing peroxidases reveal a beta-barrel fold with a conserved heme-binding motif. Proteins 69, 223-233.